NASA/CR-2007-214885/VOL3

Hypervelocity Impact (HVI)

Volume 3: WLE Small-Scale Fiberglass Panel Flat Target C-1

Michael R. Gorman and Steven M. Ziola
Digital Wave Corporation, Englewood, Colorado

September 2007

The NASA STI Program Office . . . in Profile

Since its founding, NASA has been dedicated to the advancement of aeronautics and space science. The NASA Scientific and Technical Information (STI) Program Office plays a key part in helping NASA maintain this important role.

The NASA STI Program Office is operated by Langley Research Center, the lead center for NASA's scientific and technical information. The NASA STI Program Office provides access to the NASA STI Database, the largest collection of aeronautical and space science STI in the world. The Program Office is also NASA's institutional mechanism for disseminating the results of its research and development activities. These results are published by NASA in the NASA STI Report Series, which includes the following report types:

- TECHNICAL PUBLICATION. Reports of completed research or a major significant phase of research that present the results of NASA programs and include extensive data or theoretical analysis. Includes compilations of significant scientific and technical data and information deemed to be of continuing reference value. NASA counterpart of peer-reviewed formal professional papers, but having less stringent limitations on manuscript length and extent of graphic presentations.

- TECHNICAL MEMORANDUM. Scientific and technical findings that are preliminary or of specialized interest, e.g., quick release reports, working papers, and bibliographies that contain minimal annotation. Does not contain extensive analysis.

- CONTRACTOR REPORT. Scientific and technical findings by NASA-sponsored contractors and grantees.

- CONFERENCE PUBLICATION. Collected papers from scientific and technical conferences, symposia, seminars, or other meetings sponsored or co-sponsored by NASA.

- SPECIAL PUBLICATION. Scientific, technical, or historical information from NASA programs, projects, and missions, often concerned with subjects having substantial public interest.

- TECHNICAL TRANSLATION. English-language translations of foreign scientific and technical material pertinent to NASA's mission.

Specialized services that complement the STI Program Office's diverse offerings include creating custom thesauri, building customized databases, organizing and publishing research results ... even providing videos.

For more information about the NASA STI Program Office, see the following:

- Access the NASA STI Program Home Page at ***http://www.sti.nasa.gov***

- E-mail your question via the Internet to help@sti.nasa.gov

- Fax your question to the NASA STI Help Desk at (301) 621-0134

- Phone the NASA STI Help Desk at (301) 621-0390

- Write to:
  NASA STI Help Desk
  NASA Center for AeroSpace Information
  7115 Standard Drive
  Hanover, MD 21076-1320

NASA/CR-2007-214885/VOL3

Hypervelocity Impact (HVI)

Volume 3: WLE Small-Scale Fiberglass Panel Flat Target C-1

Michael R. Gorman and Steven M. Ziola
Digital Wave Corporation, Englewood, Colorado

National Aeronautics and
Space Administration

Langley Research Center
Hampton, Virginia 23681-2199

Prepared for Langley Research Center
under Contract NNL05AC19T

September 2007

Available from:

NASA Center for AeroSpace Information (CASI)
7115 Standard Drive
Hanover, MD 21076-1320
(301) 621-0390

National Technical Information Service (NTIS)
5285 Port Royal Road
Springfield, VA 22161-2171
(703) 605-6000

Hypervelocity Impact (HVI)

Volume 3: WLE Small-Scale Fiberglass Panel Flat Target C-1

During 2003 and 2004, the Johnson Space Center's White Sands Testing Facility in Las Cruces, New Mexico conducted hypervelocity impact tests on the space shuttle wing leading edge.

Hypervelocity impact tests were conducted to determine if Micro-Meteoroid/Orbital Debris impacts could be reliably detected and located using simple passive ultrasonic methods.

The objective of Target C-1 was to study hypervelocity impacts on the reinforced carbon-carbon (RCC) panels of the Wing Leading Edge. Fiberglass was used in place of RCC in the initial tests.

Impact damage was detected using lightweight, low power instrumentation capable of being used in flight.

Table of Contents

List of Figures

List of Tables

Hypervelocity Impact (HVI)
Volume 3: WLE Small-Scale Fiberglass Panel Flat Target C-1

Introduction

In the wake of the Columbia accident, NASA personnel decided to test the idea that impacts during space flight could be detected by acoustical sensors at ultrasonic frequencies. The substance of this idea rested on the knowledge that in laboratory experiments lower velocity impacts had created signals with frequencies in the 20 – 200 kHz range. If Shuttle engine and aerodynamic noise were down in the sonic range then locating impacts would be easier in the 20-200 kHz range. The questions were what frequencies would be created during hypervelocity impacts by tiny objects, what would their energies be, and what would be the best way to detect them, keeping in mind the potential need for lightweight, simple installation procedures and low electrical energy consumption.

A further basis for selecting this method was that recent fundamental research had elucidated the basic physics of the ultrasonic signals created by the impacts in a variety of aerospace materials and geometries. This made it more likely that signal and noise could be separated and that subsequent analysis of the signals would yield the desired information about impact severity and location. All of the above reasoning proved to be correct. Hypervelocity impact by tiny aluminum spheres created signals in the 20-200 kHz frequency range easily detectable with small piezoelectric sensors similar to equipment being flown.

Target C-1 was one of several targets (see below) used for hypervelocity impact testing. There is a section in this Report for each of the other targets. The structure of this report includes a General Introduction that contains the overall goals, the personnel involved, the test methods, instrumentation, calibration, and overall results and conclusions. Only abbreviated descriptions of the test methods, instrumentation, and calibration are given in each of the Target sections such as this one.
This section describes Target C-1, the test equipment, features tables of kinetic energy and damage results, and discusses the linear relationship between kinetic energy, ultrasonic wave signal energy and damage. Also discussed are wave propagation effects, the wave modes and their velocities, and location of impacts by analysis of wave arrival times.

The Appendix has test condition data sheets, impact waveforms, and photos of the damage for each shot. Also included are tables of impact data, gain settings, recorded wave signals, and damage results.

The number of targets tested in the overall HVI study was extensive as shown in the list below:

- A-1 – Fiberglass plate and aluminum plate with standoff rods (with grommets)

- A-2 – Fiberglass plate and aluminum plate with standoff rods (no grommets)
- B-1 –Two fiberglass plates and aluminum plate with standoff rods
- C-1 – Fiberglass flat plate
- C-2 – Fiberglass flat plate
- Fg(RCC)-1 – Fiberglass in the shape of Wing Leading Edge
- Fg(RCC)-2 – Fiberglass in the shape of Wing Leading Edge
- RCC16R – Carbon-Carbon Actual WLE
- A-1 Tile – Tile structure of forward part of wing with no gap filler
- Ag-1 Tile – Tile structure of forward part of wing with gap filler
- B-1 Tile – Tile structure of aft part of wing with no gap filler
- Bg-1 Tile – Tile structure of aft part of wing with gap filler

It is everyday experience that when a solid material is struck, sound is created. This new passive ultrasonic technique has been designated modal acoustic emission (MAE) due to its (physical) similarity to an older, but less robust technique known as acoustic emission. In structures built of plate-like sections (aircraft wings, fuselages, etc.) the sound waves of interest are the extensional mode (in-plane stretching and compressing of the plate) and the flexural mode (bending of the plate). These are called plate waves and they propagate in bounded media where the wavelength of the wave is larger than the thickness of the plate. The frequency spectrum typically ranges from the low kilohertz to about one megahertz. Plate waves can be detected with simple piezoelectric transducers that convert mechanical motion into electrical voltage.

By analyzing mode shapes, and taking into account the material and loading, sources can be identified and located. The direct connection to fundamental physics is a key characteristic of MAE. For simple geometries the wave shapes and velocities have been calculated from wave equations derived from Newton's laws of motion and they compare well with measurements. (See General Introduction to this report for a fuller discussion of modal AE.) By using arrival times at transducers with known positions, the location of the source can be triangulated by various mathematical methods (similar to methods used in SONAR).

Experimental Description

Target C-1 consisted of a 34" x 34" 20-ply fiberglass panel (Figure 1). L-shaped angles added to the back of the fiberglass panel were used to attach the target to a target support stand.

Figure 1: Fiberglass Panel Target C-1. Front View.

There were a total of 19 shots fired. The impact angle of the shots was 90 degrees from the surface of the target for shots #1 - 10 and 45 degrees for shots #11 - 19 (Figure 2 and Figure 3).

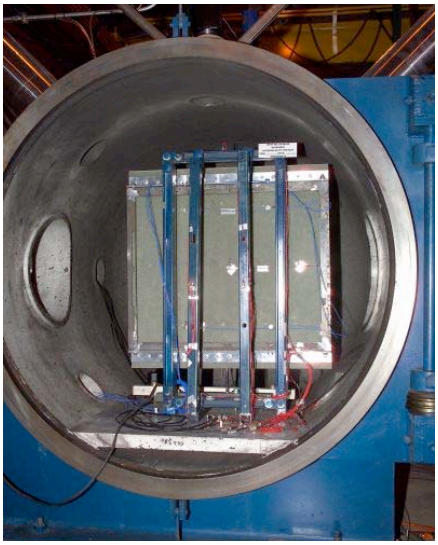

Figure 2: Fiberglass Panel Target C-1 with 90 deg Impact Angle. Back Side View.

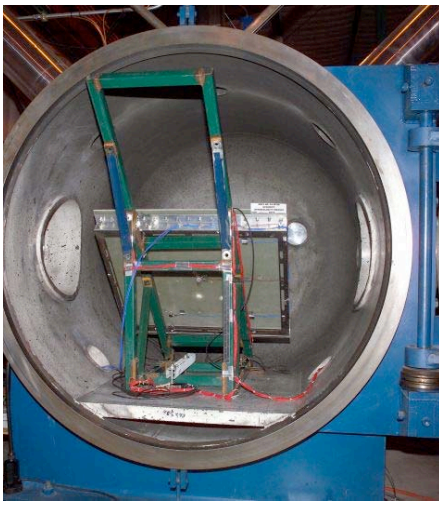

Figure 3: Fiberglass Panel Target C-1 with 45 deg Impact Angle. Back side View.

The tests were conducted on the 0.50 caliber hypervelocity launcher range at the White Sands Test Facility (WSTF). The flight range for the hypervelocity projectile and target chamber were evacuated to near vacuum pressure (6-8 Torr) prior to each shot. The AE recording equipment was connected by feed-throughs to the sensors on the target inside the vacuum chamber. The connectors were BNC type.

The projectiles were small spheres made of 2017 T-4 aluminum. They ranged in diameter from 0.4 mm to 2.4 mm. Impact velocity was measured with WSTF diagnostic equipment on each shot. The projectile kinetic energy for these shots ranged from 2.18 J to 461.19 J.

Four acoustic (ultrasonic) emission sensors were coupled to the back of the target with Lord 202 acrylic adhesive (Figure 4). A diagram of the sensor layout is shown in Figure 5. A photo of the sensor layout is shown in Figure 6.

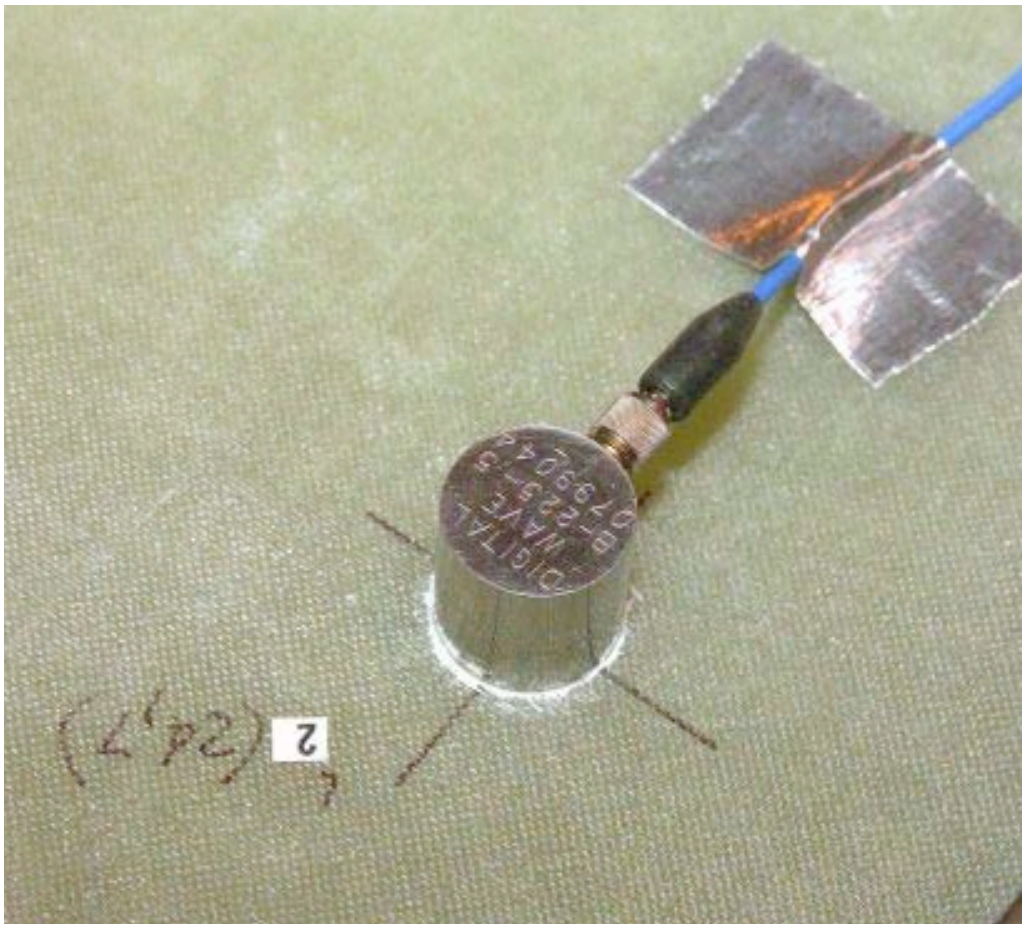

Figure 4: C-1 Detail of Sensor 2

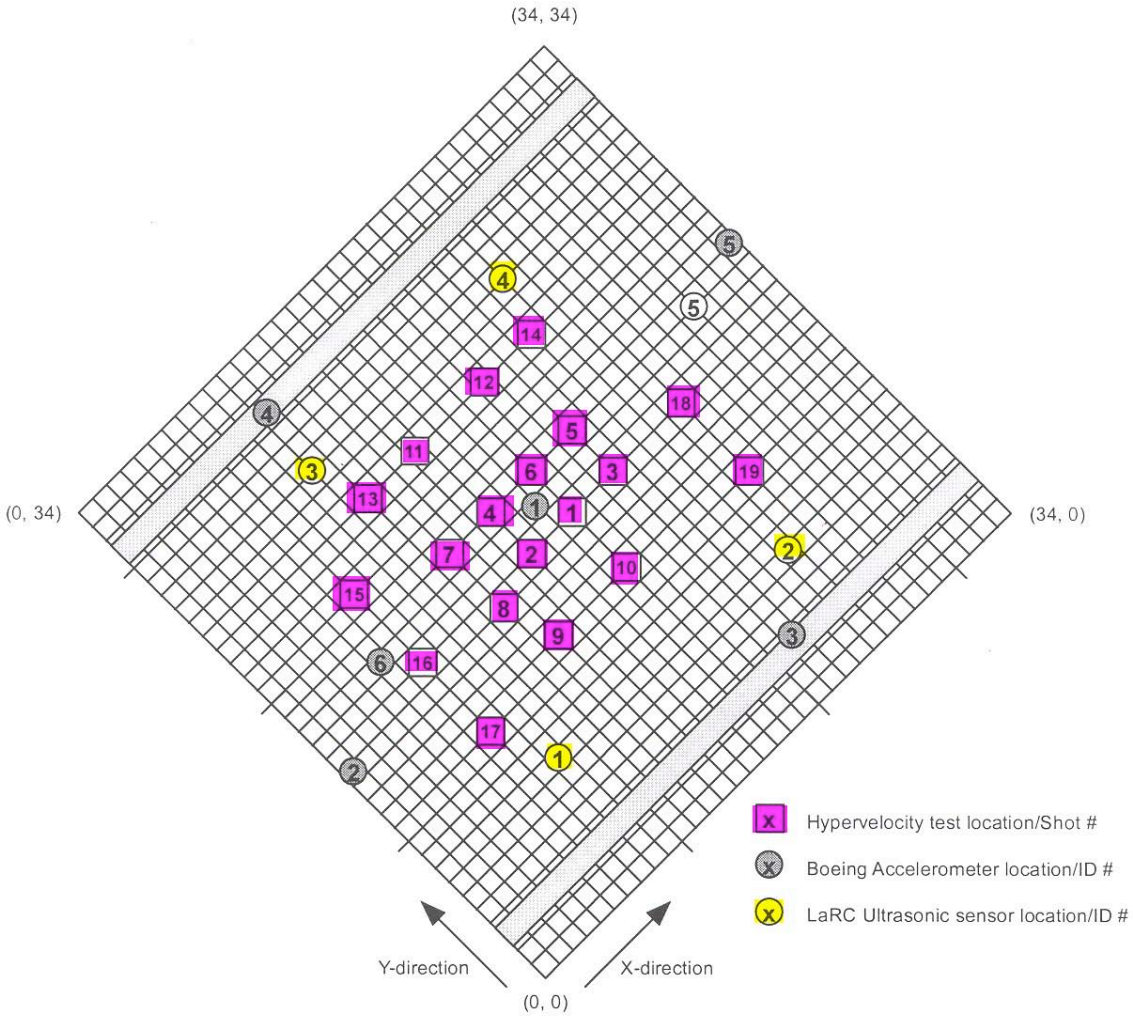

Figure 5: C-1 Diagram of Sensor and Impact Locations. Front View.

Acoustic emission sensors are highlighted in yellow with the following coordinates: #1(10, 7), #2 (24, 7), #3 (10, 27), #4 (24, 27). Dimensions are in inches.

Impact locations are highlighted in magenta with the following coordinates: #1 (18, 16), #2 (15, 16), #3 (21, 16), #4 (15, 19), #5 (21, 19), #6 (18, 19), #7 (12, 19), #8 (12, 15), #9 (13, 12), #10 (17.5, 12), #11 (14.5, 24), #12 (19.5, 24), #13 (11, 24), #14 (23, 24), #15 (7, 21), #16 (7, 16), #17 (7, 11.25), #18 (26, 16), #19 (26, 11.5)

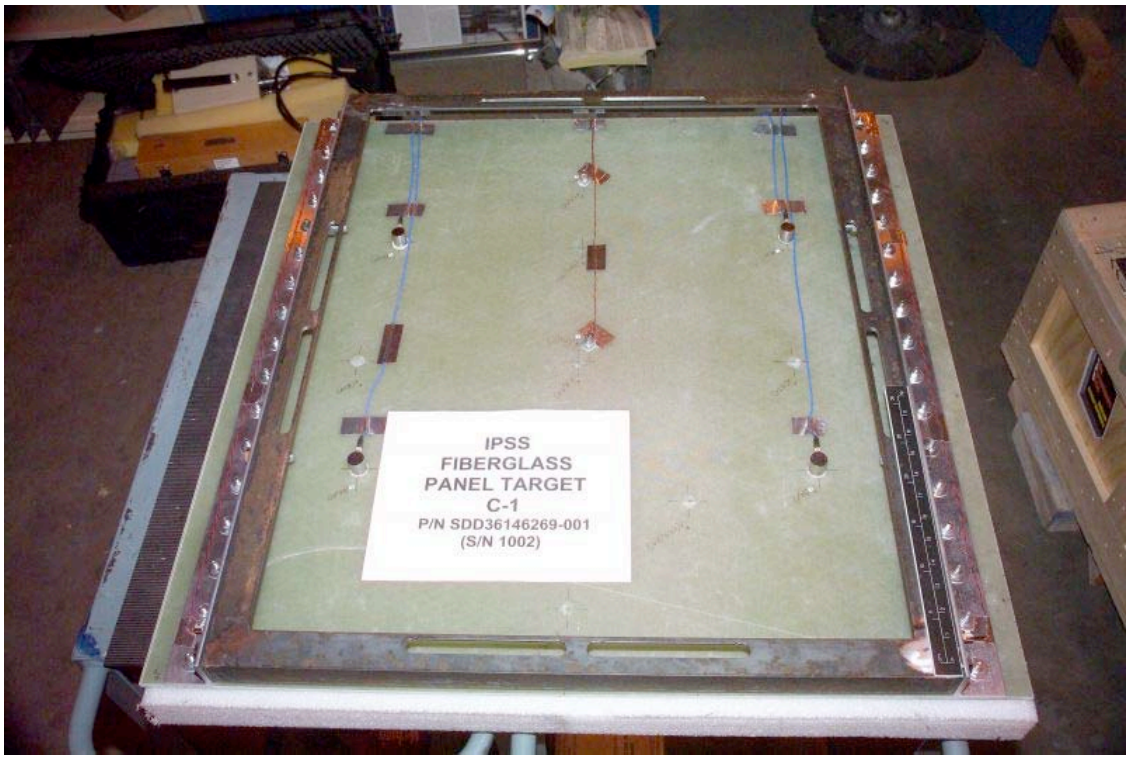

Figure 6: C-1 Photo of Sensor Locations

The piezoelectric sensors converted the sound wave energy to electrical voltages. The energy computed from the voltage data collected by each sensor channel is referred to as the wave signal energy. (A complete description of the type of sensor used and calibration is given in the General Introduction to this report.)

The wave signal energy for each channel was analyzed and compared to the impact energy. A full description of the wave recording instrumentation is given in the General Introduction to this Report. (Each individual sensor was connected to a separate amplification and filtering channel and the voltage produced by the sensor recorded and stored on a computer.)

The wave signal energy was computed by integrating the squared voltage with respect to time and dividing this number by the impedance at the preamp input. The voltage versus time values of the wave, which were displayed in the waveform window on the computer screen for each channel, were not corrected for any applied gain (or attenuation).

Attenuation was the norm because hypervelocity impact produced very energetic signals that in most cases would have saturated the A/D converter on the recording card in the computer had the amplitude not been reduced.

Some recorder channels were found to have a slight DC offset (Figure 7). This added significantly to the wave energy when the integral of squared voltage versus time signal

was computed. To eliminate the offset, the average wave signal voltage for the impact event was subtracted from each data point. This resulted in a zeroed raw wave signal (no DC offset. Correcting the offset was more important for small signals than large signals.

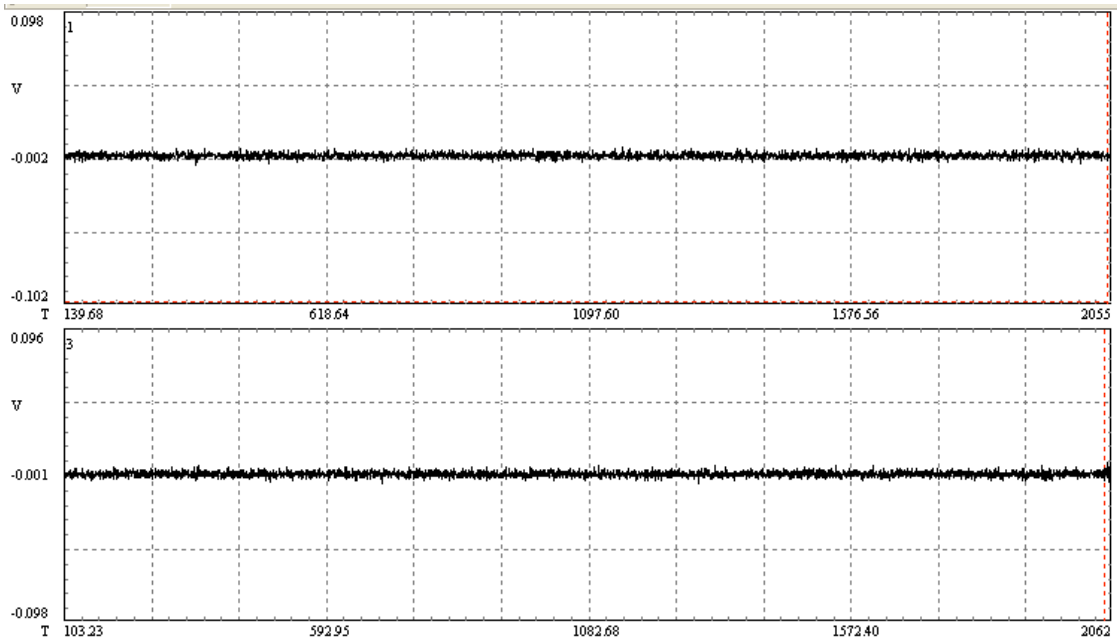

Figure 7: Example of DC Offset

The top signal is centered at -0.002 V whereas the bottom signal is centered at -0.001V.

A typical impact signal is shown in Figure 8. The impact signal had a distinct waveform and varied in both in arrival time and amplitude on each channel. The distinct modal characteristics can be seen in a time expanded view in Figure 9. The E mode arrived first with its lowest frequency in front followed by progressively higher frequencies. This was followed by the flexural (F) wave. The F wave characteristics were harder to discern because of the filtering of the attenuators. In some cases, the F wave characteristics are much more visible (See Figure 18 to compare with a pencil lead break. A pencil lead break created a much larger F mode than E mode.) The vastly different velocities of the modes were used to confirm the modes.

The sound waves produced by impact are shown complete in the Appendix. It can be seen that the impact waves have the plate mode characteristics, i.e., the extensional wave arrives first, with its low frequency components out front followed by higher frequency components, and the F wave with just the opposite frequency arrangement. This differs, for example, from noise caused by electromagnetic interference (EMI). In contrast, EMI noise typically looks the same on every channel and arrives simultaneously (Figure 10). EMI exhibits no plate wave propagation characteristics.

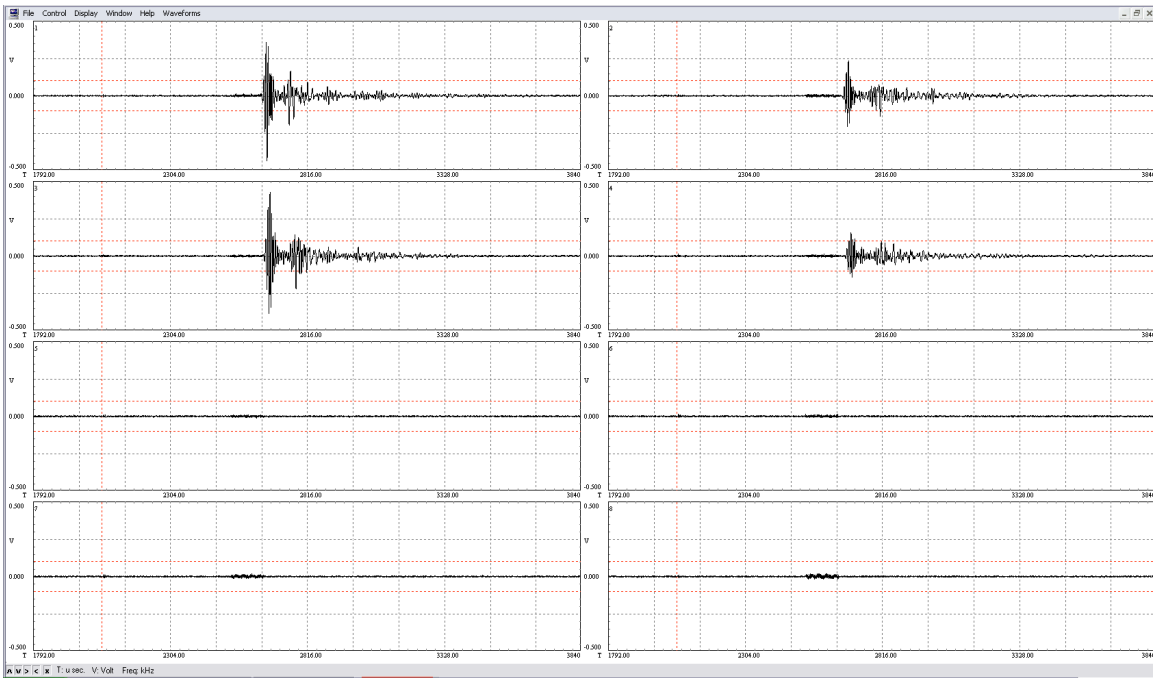

Figure 8: C-1 Impact Signal for Shot #2b

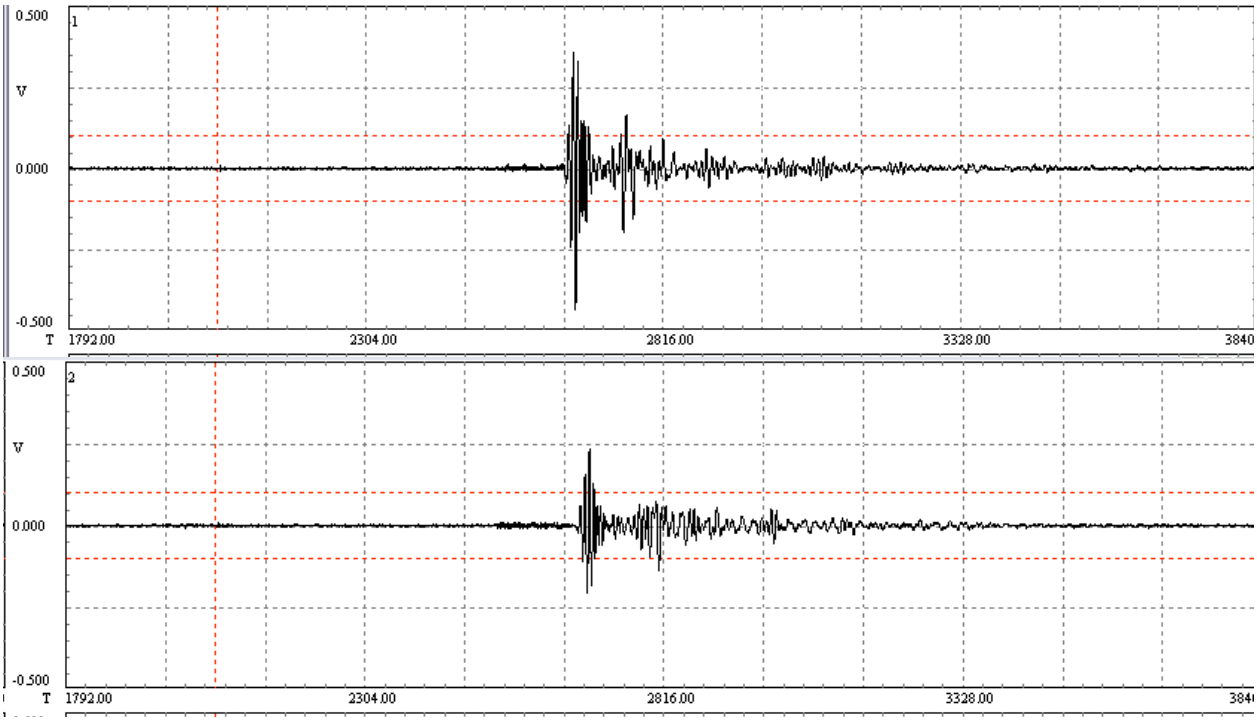

Figure 9: Detail of C-1 Impact Signal for Shot #2b, Sensors 1 and 2

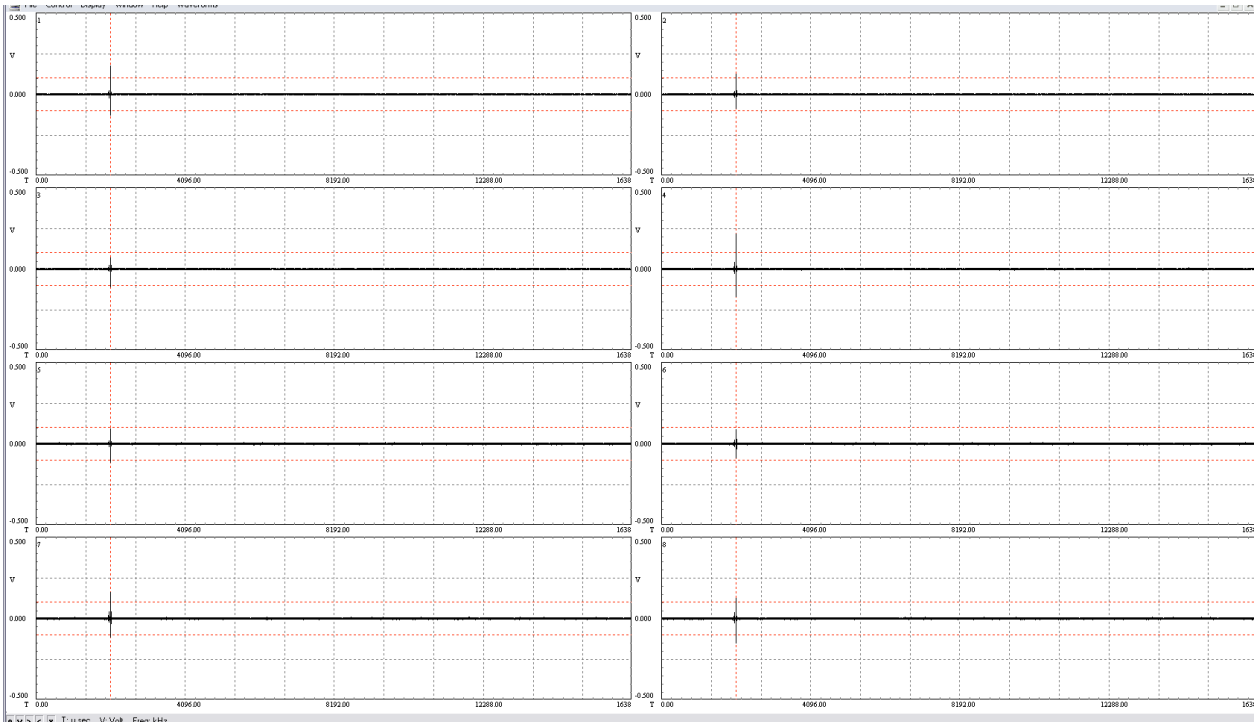

Figure 10: C-1 Electromagnetic Interference for Shot #2b

The MAE software computed the raw wave signal energy in Joules uncorrected for any analog gain or attenuation that may have been applied to the signal path. In order to compare the wave energies from shot to shot, the raw wave signal energy was converted by applying Equation 1 where E_{raw} is the energy computed using the recorded wave (with DC offset eliminated) and G is the system gain.

$$W.S.E. = \frac{E_{raw}}{G^2} \qquad \textbf{Equation 1}$$

The gain G was computed by converting the logarithmic gain, M, in decibels with Equation 2 or Equation 3.

$$M\ dB = 20\ Log_{10}\ (G) \qquad \textbf{Equation 2}$$

$$G = 10^{\frac{M}{20}} \qquad \textbf{Equation 3}$$

The gains, raw wave signals, and wave energies for each shot are listed in the data tables in the Appendix to this section.

High velocity impact produced signals on the order of a few volts directly out of the transducer. These were much larger signals than typically found in most acoustic emission measurements of, say, crack growth in metals. For most shots, attenuators were placed in the signal lines between the sensors and the digital recorders. Greater attenuation was applied for the higher energy shots which made the raw energy appear to be much less. The energy was restored to its full value by compensating in the analysis for the greater attenuation, Equation 3 above.

Results

The most important quantities used in the analysis of the wave signals were the wave signal energy and projectile kinetic energy for each shot. These are given in Table 1 along with the test number, impactor diameter, and angle of impact. Wave signal energy is the sum of the energy, in nano-Joules, detected by all of the sensors. Kinetic energy is calculated based on the velocity and mass of projectile (density of aluminum = 2700 kg/m^3) according to the usual formula K.E. = $mv^2/2$.

For design engineering and threat analysis purposes, shots were performed at various angles to the normal to the target at the point of impact. It was suggested by Summers (NASA TN D-94, 1959) that only the normal kinetic energy be used to compare with crater depth. The kinetic energy for the normal velocity component was computed (sine squared of the angle, ninety degrees is normal). Normal KE is just the kinetic energy associated with the projectile velocity component normal to the target surface at the point of impact.

As can be seen in Figure 11 and Figure 12, the normal kinetic energy correlated better than the total kinetic energy with damage area.

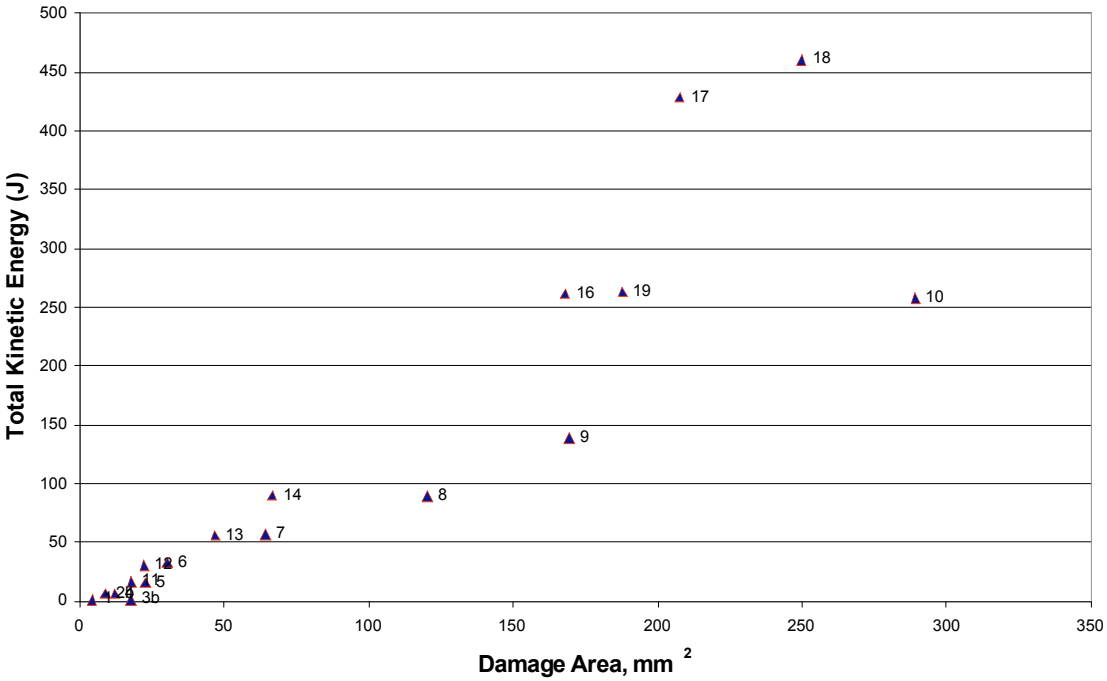

Figure 11: C-1 Total Kinetic Energy vs. Fiber Damage Area

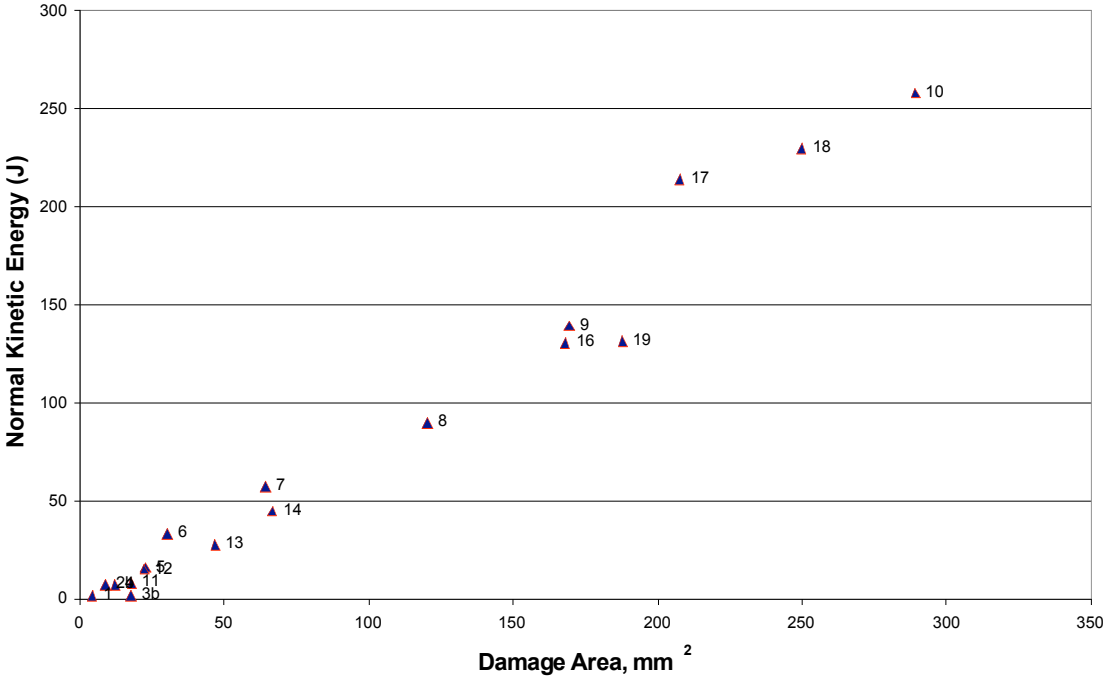

Figure 12: C-1 Normal Kinetic Energy vs. Fiber Damage Area

In Figure 13 and Figure 14, the total kinetic energy correlates with crater volume damage better than the normal kinetic energy.

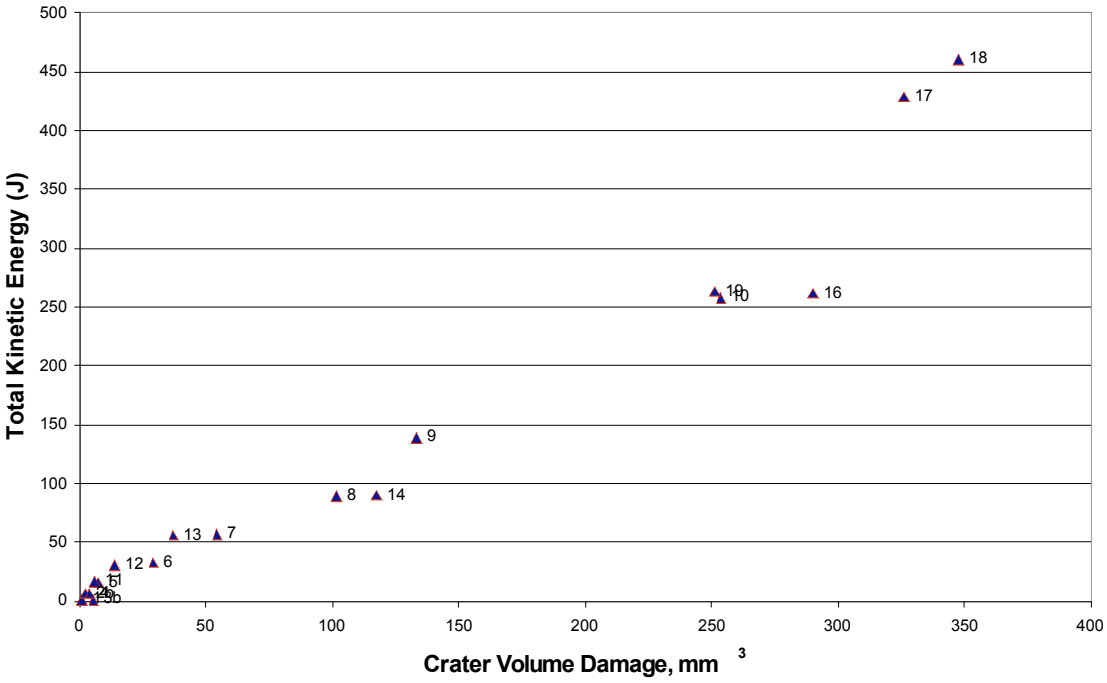

Figure 13: C-1 Total Kinetic Energy vs. Crater Volume Damage

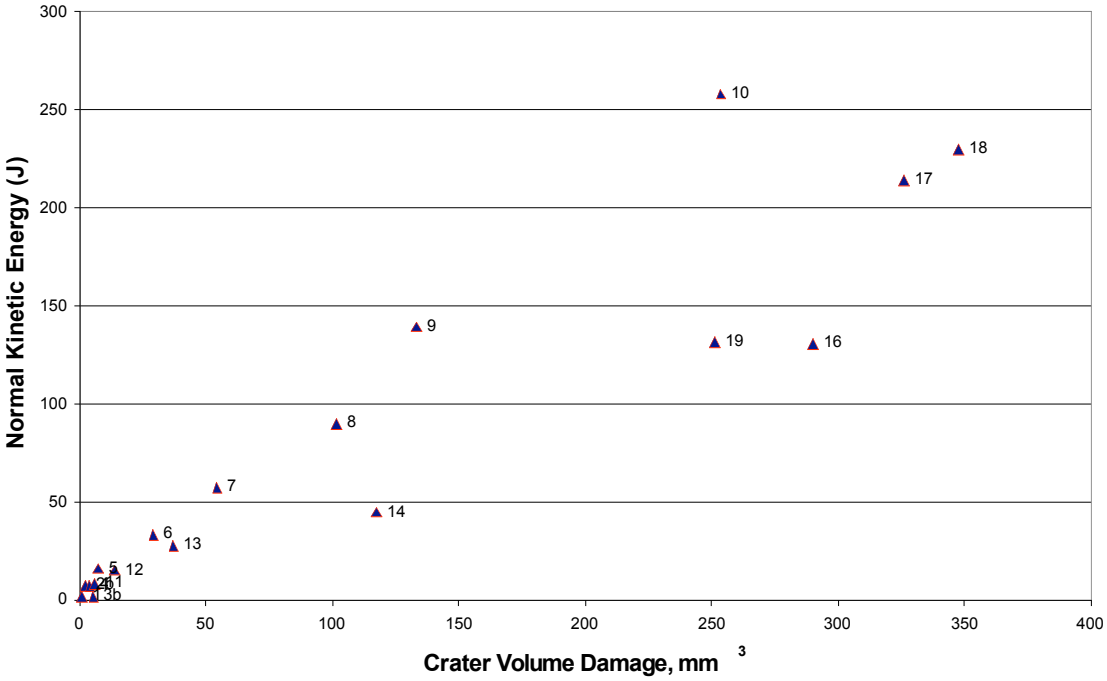

Figure 14: C-1 Normal Kinetic Energy vs. Crater Volume Damage

Wave signal energy correlates with normal kinetic energy better than with total kinetic energy as can be seen in Figure 15 and Figure 16.

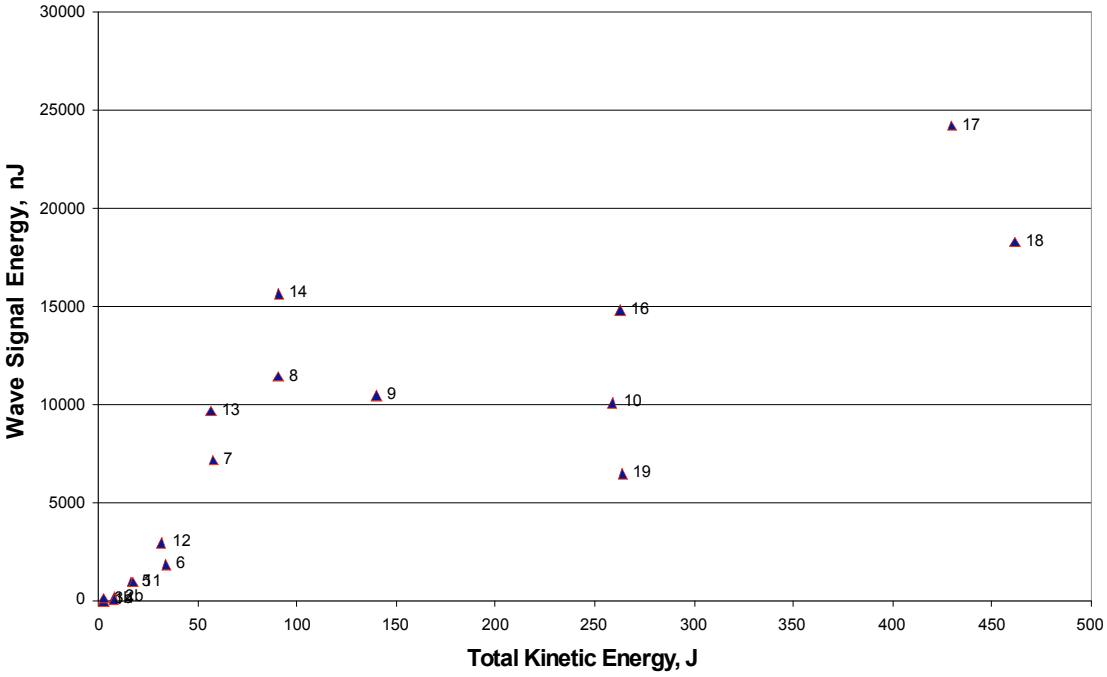

Figure 15: C-1 Wave Signal Energy vs. Total Kinetic Energy

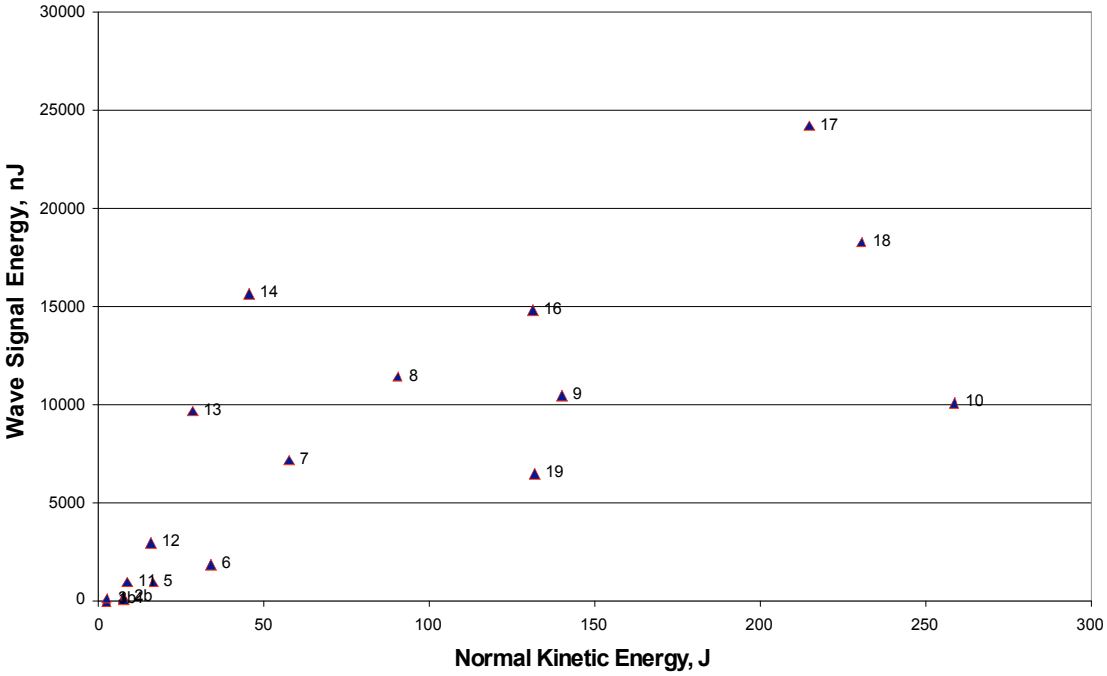

Figure 16: C-1 Wave Signal Energy vs. Normal Kinetic Energy

	Imp Dia	Imp Ang	Normal K. E.	Total K.E.	W.S.E.
Test No.	mm	deg	J (± 5%)	J (± 5%)	nJ
C1-1	0.4	90	2.18	2.18	1.41E+01
C1-2b	0.6	90	7.48	7.48	2.01E+02
C1-3b	0.4	90	2.18	2.18	1.43E+02
C1-4	0.6	90	7.42	7.42	1.09E+02
C1-5	0.8	90	16.34	16.34	1.00E+03
C1-6	1.0	90	33.75	33.75	1.89E+03
C1-7	1.2	90	57.48	57.48	7.23E+03
C1-8	1.4	90	90.22	90.22	1.15E+04
C1-9	1.6	90	139.85	139.85	1.05E+04
C1-10	2.0	90	258.41	258.41	1.01E+04
C1-11	0.8	45	8.63	17.28	1.01E+03
C1-12	1.0	45	15.57	31.17	2.97E+03
C1-13	1.2	45	28.22	56.48	9.73E+03
C1-14	1.4	45	45.20	90.48	1.57E+04
C1-16	2.0	45	68.87	137.85	1.49E+04
C1-17	2.4	45	131.02	262.25	2.43E+04
C1-18	2.4	45	214.59	429.53	1.83E+04
C1-19	2.0	45	230.41	461.19	6.51E+03

Table 1: C-1 Kinetic Energy and Wave Signal Energy

Test No. C1-15 is not included in the results because the signals were not acquired since the instrument was not in record mode. The data sheet for shot #3b lists a projectile diameter of 0.4 mm yet the Test Results list a projectile diameter of 0.6 mm.

The damage for each shot is given in Table 2. The crater volume damage is the product of the recorded length, width, and depth measurements on the front side of the panel for each impact. Damage area is the product of recorded length and width measurements of the fiber damage on the front side of the panel. Figure 17 is a photograph of the damage created by shot #8.

	Normal K. E.	Total K.E.	Damage Area	Crater Volume
Test No.	J	J	mm^2	mm^3
C1-1	2.18	2.18	4.0	0.46
C1-2b	7.48	7.48	8.8	2.1
C1-3b	2.18	2.18	17.5	5.1
C1-4	7.42	7.42	12.0	3.6
C1-5	16.34	16.34	22.5	6.8
C1-6	33.75	33.75	30.0	28.9
C1-7	57.48	57.48	64.0	54.0
C1-8	90.22	90.22	120.0	101.3
C1-9	139.85	139.85	169.0	132.7*
C1-10	258.41	258.41	289.0	253.4*
C1-11	8.63	17.28	17.6	5.5
C1-12	15.57	31.17	22.1	13.5
C1-13	28.22	56.48	46.6	36.7
C1-14	45.20	90.48	66.3	117.0
C1-16	68.87	137.85	167.7	289.6*
C1-17	131.02	262.25	207.3	325.8*
C1-18	214.59	429.53	249.5	347.5*
C1-19	230.41	461.19	187.6	251.0*

Table 2: C-1 Damage Results.
*=Hole.

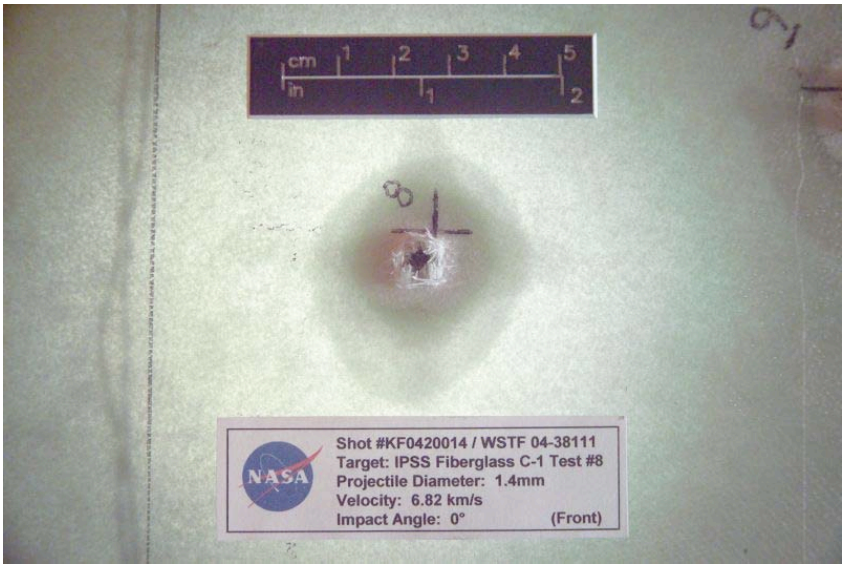

Figure 17: C-1 Impact Damage Area for Shot #8

Discussion

Sound waves containing both sonic and ultrasonic frequencies were created by each impact. The energy in the waves is some fraction of the energy of the impactor. An analysis method was sought that would allow a straightforward and simple technique for comparing the wave energies to the projectile kinetic energy, and thus the damage figures. One way would be to look at the energy sensor by sensor. For example, the wave energy for shot #1 could be computed from just the signal at sensor 1, then the energy from shot #2 could be computed from the signal at sensor 1, and so forth, and then the energies could be graphed.

The problem with this method would be that the impact position changed from shot to shot. The method might work if new identical targets were available each time and the sensor 1 position and shot location were always the same. Given this was not feasible, perhaps correction factors could be developed, but it would be arduous, if not impossible, to compare shot energies by correcting for the all the source to receiver relative positional changes because there are so many effects for which to account. Geometric spreading in 3-D means that the intensity varies as $1/r^2$. In plates the spreading is circular and the intensity only drops as 1/r. Calculating the 1/r attenuation caused by geometric spreading would account for just one effect. There is also attenuation due to material properties which is a function of both frequency and direction. Waves that cut across the main fiber directions were attenuated more than waves that propagated along the fiber directions. This is known as material anisotropy.

In order to reduce the effect of varying impact positions on the acoustical energy values, the energies of the waves at all the transducers on the target were summed together for each shot. This was approach was based on the following reasoning: If a given sensor records the signals for two impacts that have the same kinetic energy, the closer impact would appear to have a larger wave signal energy. Since the sensors surrounded the impacts, variations in the propagation paths would be roughly accounted for by adding the wave signal energy collected by all sensors. This approach also makes use of symmetry: Two symmetric impacts would have symmetric propagation paths and thus the same total wave signal energy if the energies collected by all the sensors were summed. The graphs show that this turned out to be an efficacious approach. Symmetry could not be invoked in every case so there were outliers.

The damage measurements themselves were crude. Although some damage in the interior plies seemed apparent, the “damage area” value that was plotted against KE was related solely to the area the damaged fibers occupied as measured with a ruler on the outside (the impact side) surface.

Overall, the correlations exhibited the correct trend of greater impact energy resulting in larger wave energy.

Location Analysis

Location of the source of a wave is part and parcel of the MAE technique just as it is in SONAR methods. It contributes to understanding of the type and magnitude of the source and is a crucial step in tracking down and stopping leaks in manned spacecraft.

In these studies the location of the impact was known by visual observation. This enabled a study of the accuracy of locating a source purely by analysis of the wave arrival at different transducers. The source position was triangulated when the source to receiver path was reasonably homogeneous. This was shown in detail for Target Fg(RCC)-1 and the reader is referred to that Section of this Report. The analysis was not repeated here.

The velocities of the direct arrivals were measured in advance. Pencil lead breaks were done to create the modes. This is discussed under Wave Propagation below.

Wave Propagation

The wave signal energy collected by any given sensor is composed of direct energy and reflected energy. After an impact occurs, a wave propagates radially outward from the impact site. This direct wave is the first signal recorded by a sensor. When this wave reaches the edges of the target, it is reflected back to the sensor. These reflected waves are lower in amplitude than the direct waves and have later arrival times. In general, reflected waves did not contribute not a significant fraction of the signal energy.

The direct wave is composed of two types of waves: extensional and flexural. Extensional waves have two displacements components with the larger displacements perpendicular to the normal to the plate. A sensor on the surface detects the out-of-plane component of the E wave. The largest displacement of the flexural wave motion is perpendicular to the plane of the plate. This motion is caused by bending at the impact location. The E and F modes have very distinct characteristics (see General Introduction and also Figure 18) that can be readily identified. For one thing, the front part of the E wave travels much faster than any frequency component of the F wave.

Wave speed was determined by performing a lead break at one sensor and measuring the time it took for a direct wave to arrive at another sensor at a known distance away. Figure 18 shows a lead break signal at sensor 1. The extensional wave arrived at sensor 1 at t_1 = 200.4 μs and at sensor 2 at t_2 = 288.4 μs. The sensors were located 14 inches apart which gave a velocity of 0.16 in/μs in the x-direction. Performing this calculation in the y-direction and the diagonal gave extensional wave velocities of 0.16 in/μs and 0.14 in/μs, respectively. Figure 19 is a diagram of the sensor layout.

Low frequency (< 50 kHz) noise did not affect signal arrival time. Examples of filtered and unfiltered waveforms are given in the Discussion section of RCC16R and in the General Introduction.

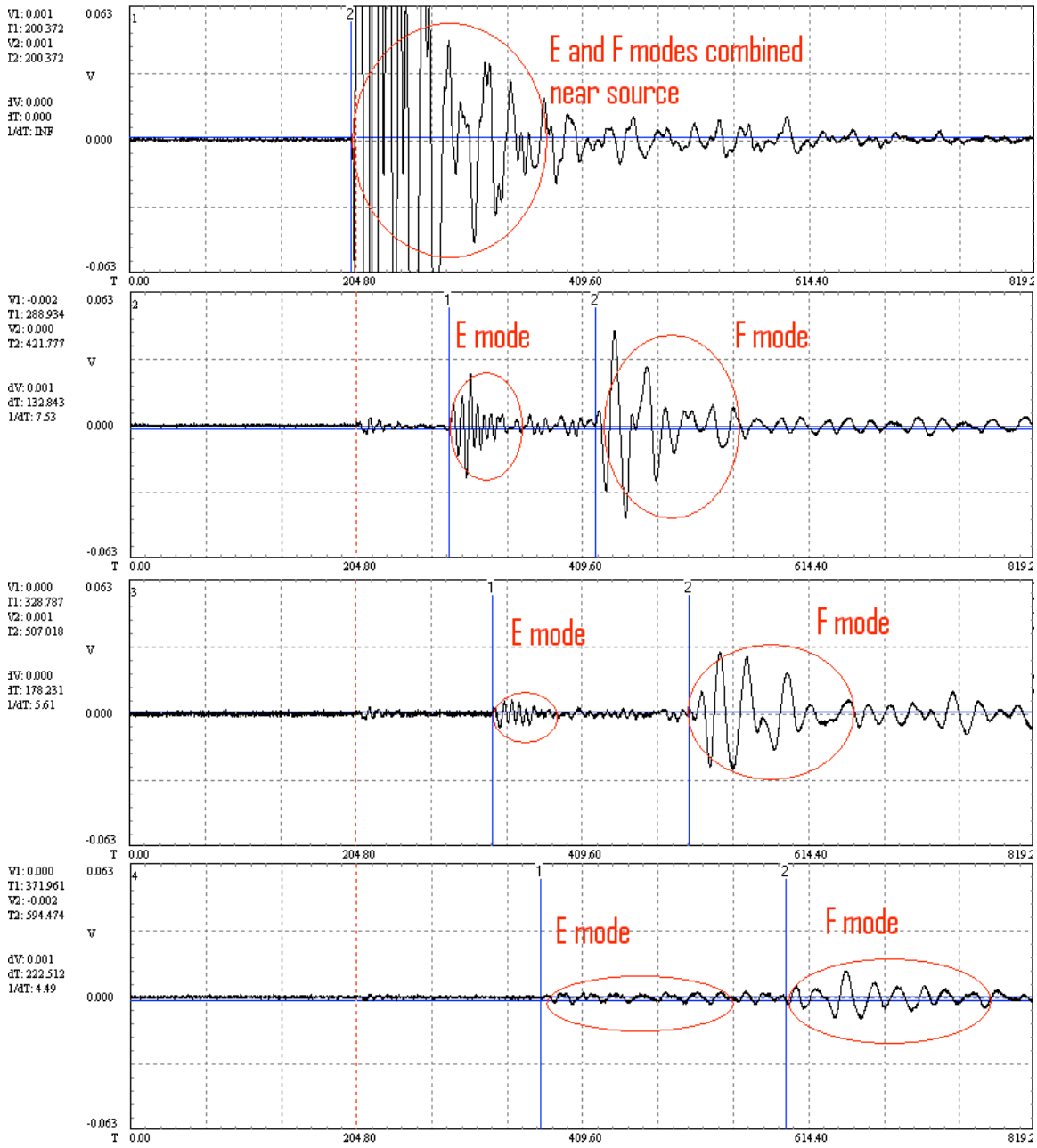

Figure 18: C-1 Lead Break Near Sensor 1 on Sensors 1, 2, 3, and 4 for Shot #1 Pretest

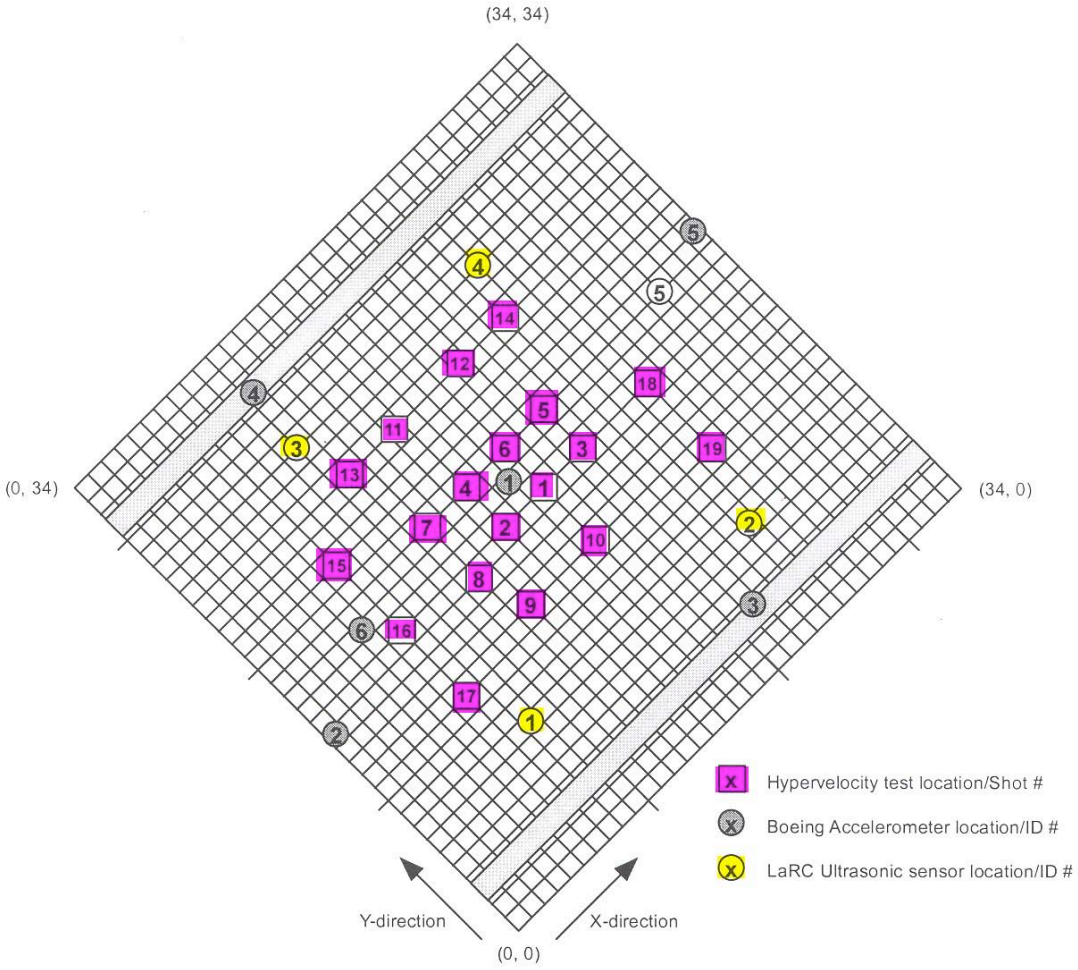

Figure 19: C-1 Diagram of Sensor Locations. Front View. (Repeat of Figure 5.)
Acoustic emission sensors are highlighted in yellow with the following coordinates:
#1(10, 7), #2 (24, 7), #3 (10, 27), #4 (24, 27).
Impact locations are highlighted in magenta with the following coordinates:
#1 (18, 16), #2 (15, 16), #3 (21, 16), #4 (15, 19), #5 (21, 19), #6 (18, 19), #7 (12, 19), #8 (12, 15), #9 (13, 12), #10 (17.5, 12), #11 (14.5, 24), #12 (19.5, 24), #13 (11, 24), #14 (23, 24), #15 (7, 21), #16 (7, 16), #17 (7, 11.25), #18 (26, 16), #19 (26, 11.5)

In the fiberglass panel, fibers are aligned in the x and y directions (see Figure 19). In addition to having slower speeds, waves that travel diagonally are attenuated more than waves that travel along the fiber direction. This is generally known as material anisotropy and is referred to here as the diagonal attenuation effect.

The data can be corrected for the effect of diagonal attenuation by scaling the wave signal energy with the angle that the sensor makes with the impact location. The scaling factor could be determined by plotting the wave signal energy for an array of sensors. Figure 20 shows a test setup for determining the amount of diagonal attenuation in a material. Each sensor is the same distance away from the impact location. If the material were

homogenous and isotropic, the wave signal energy would be the same for all sensors. If the material were orthogonally isotropic fiberglass, however, the wave signal energy would be strongest along the direction of the fibers. Thus, the wave signal energy would be largest for sensors 1 and 5 and smallest for sensor 3. The ratio of the attenuated signal to the non-attenuated signal would be the correction factor for that angle.

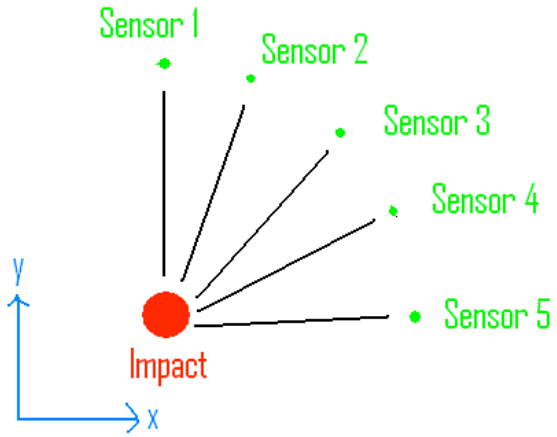

Figure 20: Sensor Array for Observing Diagonal Attenuation

An exact scaling factor for every sensor on every impact would require more effort in the present case than it would be worth, but the effect on the data of the diagonal attenuation can be approximated. It can be shown that the data points that seemed to be outliers would in fact have been more in line with the other data points in the KE plots by considering how many sensors are aligned with each impact point and fiber directions and observing that, for similar kinetic energies, the impact positions that were aligned with both fibers and sensors had the higher wave signal energies.

In the present experiment, most shots were approximately aligned with two sensors. Shots #13 and 14, however, were aligned with three sensors while shots #1-5 and 10 were aligned with none. Shot #10 was in the least preferred wave propagation position. The signals of shots #13 and 14 propagated with the least attenuation and had relatively higher energies. Shot #10 was in the least preferred wave propagation position so its energy was knocked down. Both of these results were confirmed by the plots. Rough scaling factors were determined by using the shots with similar kinetic energies and computing ratios when a given pair of shots with nearly identical kinetic energies had in common an aligned receiver position and an unaligned receiver position. The scaling factor for shot #10 was determined to be close to two. The scaling factor for shots #13 and 14 was determined to be 0.7. This shows that if the diagonal attenuation were to be taken into account that the K.E. vs. W.S.E. plot would improve as in Figure 21. The clustering of the remaining shots would also improve if the wave propagation were strictly taken into account. (The estimated wave signal energies for shots #10, 13, and 14 were 30,000 nJ, 6,000 nJ, and 10,000 nJ, respectively.)

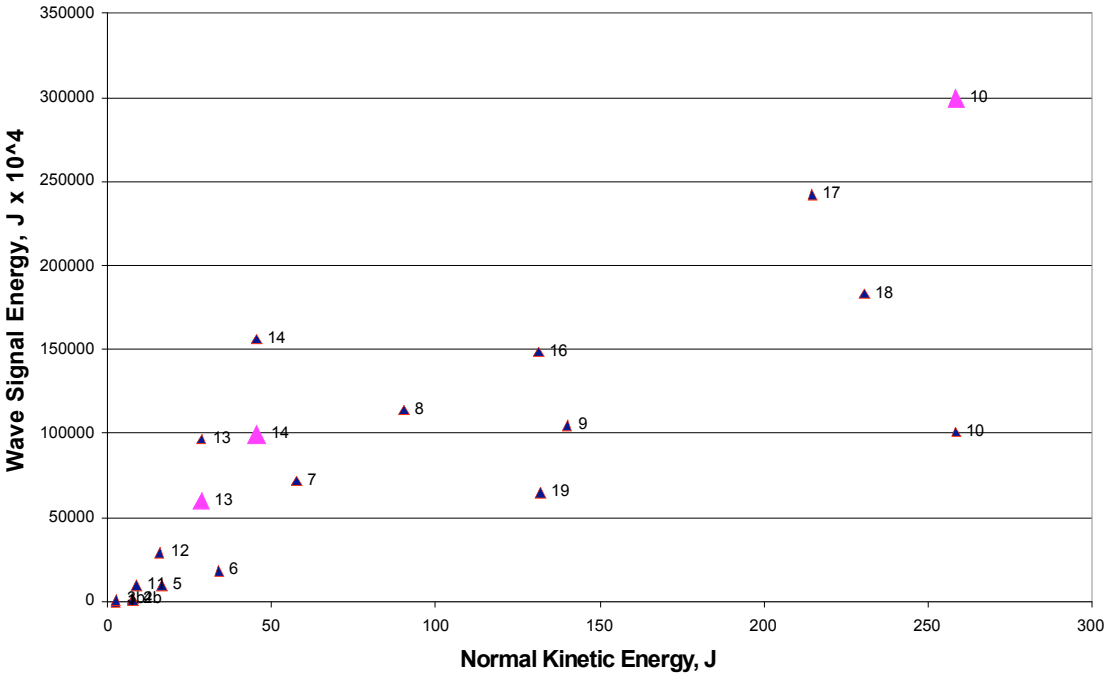

Figure 21: C-1 Normal Kinetic Energy vs. Wave Signal Energy with Shots #10, 13, and 14 Scaled for Diagonal Effects

Conclusions

The results of the hypervelocity impact test on fiberglass Target C-1 are as follows:

- Ultrasonic Sensors were successfully bonded to fiberglass Target C-1 with a Lord 202 Acrylic Adhesive.

- Ultrasonic Sensors operated well in near-vacuum (6-8 Torr) inside the vacuum chamber at Johnson Space Center's White Sands Testing Facility.[1]

- Impacts created detectable ultrasonic signals at high (>50 kHz) frequencies which should be above flight noise.[2]

- Ultrasonic signals were detected with small, lightweight sensors capable of space flight.[3][4]

- Wave propagation characteristics of the cross-ply fiberglass target were measured and used in the analysis of the wave signal energy.

- Wave signal energy correlated well with kinetic energy and impact damage.

This test successfully demonstrated the ability for a wing leading edge impact detection system (WLEIDS) to model the kinetic energy response and material damage below, at and above complete penetration of the projectile through the target.

[1] B1025 sensors also functioned well in deep vacuum of ESEM. Michael Horn, NASA LaRC, email 2005.
[2] Based on measurement of noise spectra on F16 bulkhead at full throttle, there will not be significant noise power above 50kHz.
[3] Sensors passed 18,000 g shock test. Henry Whitesel, Naval Surface Warfare Center, verbal communication 1998.
[4] DWC sensors survived intense radiation environment. Dane Spearing, LANL, verbal communication 2003.

Appendix

The appendices contain the information for each shot and the waveforms. For completeness, and, for usefulness when judging the energy versus damage plots shown in the discussion section above, tables are given at the end that summarize and group together the data for the key test variables.

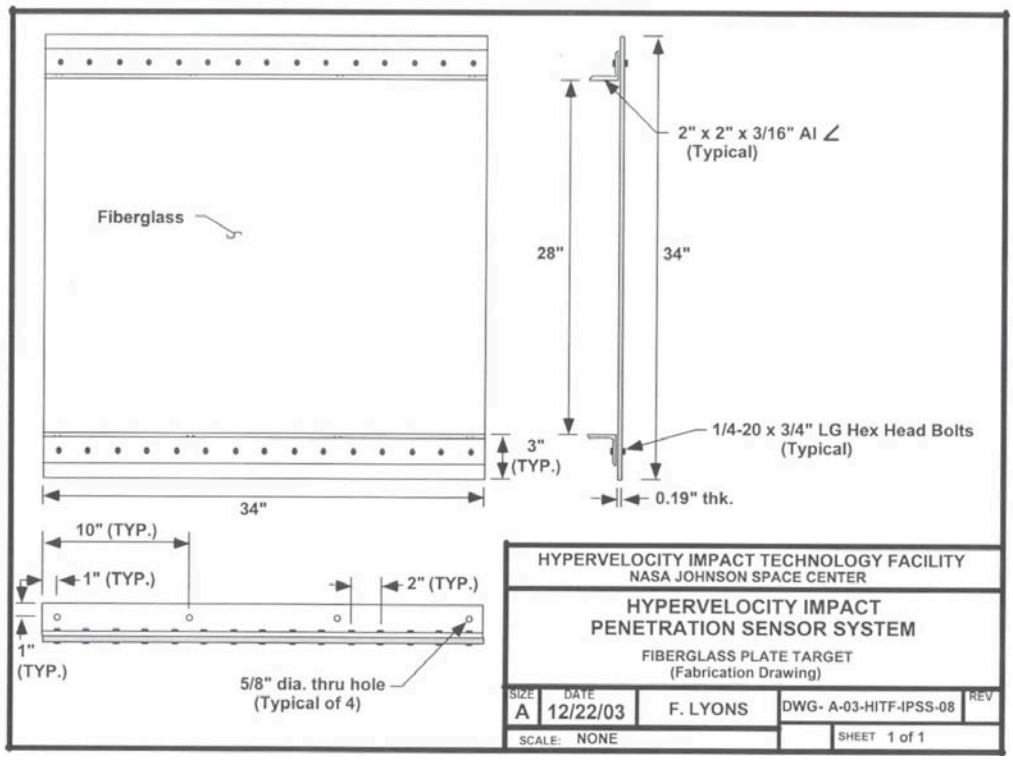

Figure 22: Fiberglass Article Target C-1 Drawing

Test Condition Data Sheets

Test conditions for AE (ultrasonic) data acquisition during hypervelocity impact testing

Test date: 1-15-04

Specimen description: Fiberglass
Target C-1
Shot # 1

Impact conditions:
Projectile material and diameter: 0.4 mm diameter aluminum
Planned impact coordinates (in.): 18, 16
Actual impact coordinates (in.): 18.2, 16.1
AE estimated impact coordinates (in.):
Planned impact velocity (km/s): 6.8
Actual impact velocity (km/s): 6.94
Impact angle: 0

Sensor information:

Ch. #	Sensor Model	x coord. (in.)	y coord. (in.)	Attenuation at sensor * (dB)	Preamp gain/ attenuation (dB)	System gain (dB)	Total gain/ attenuation (dB)
1	225	10	7	-50	0	27	-23
2	225	24	7	-50	0	27	-23
3	225	10	27	-50	0	27	-23
4	225	24	27	-50	0	27	-23

* Preliminary estimate for attenuation at sensor based on field measurements.
Attenuators calibrated for 50 ohm input, but used for high impedance preamp input.
Further laboratory characterization required.

Signal filter settings: 20kHz – 1500 kHz bandpass on all channels
Instrumentation settings:
5 MHz sampling rate
32k points
4096 pretrigger points

Comments: Good signals acquired.

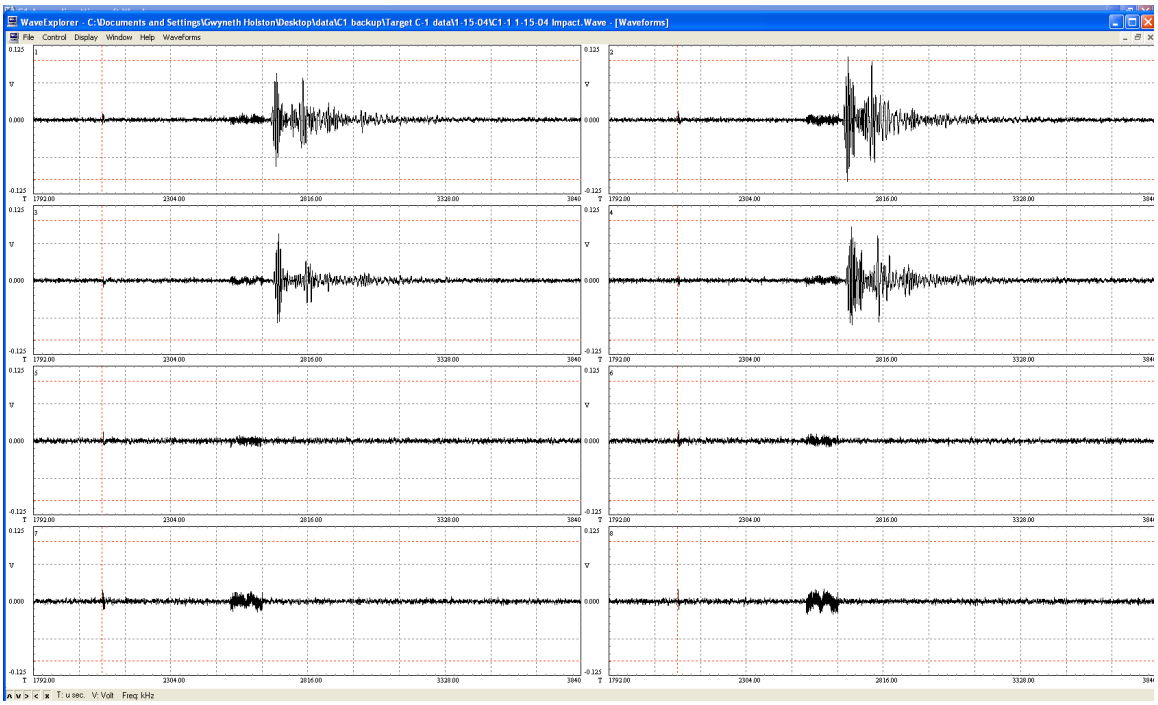

Figure 23: C-1 Shot #1 Impact Waveform

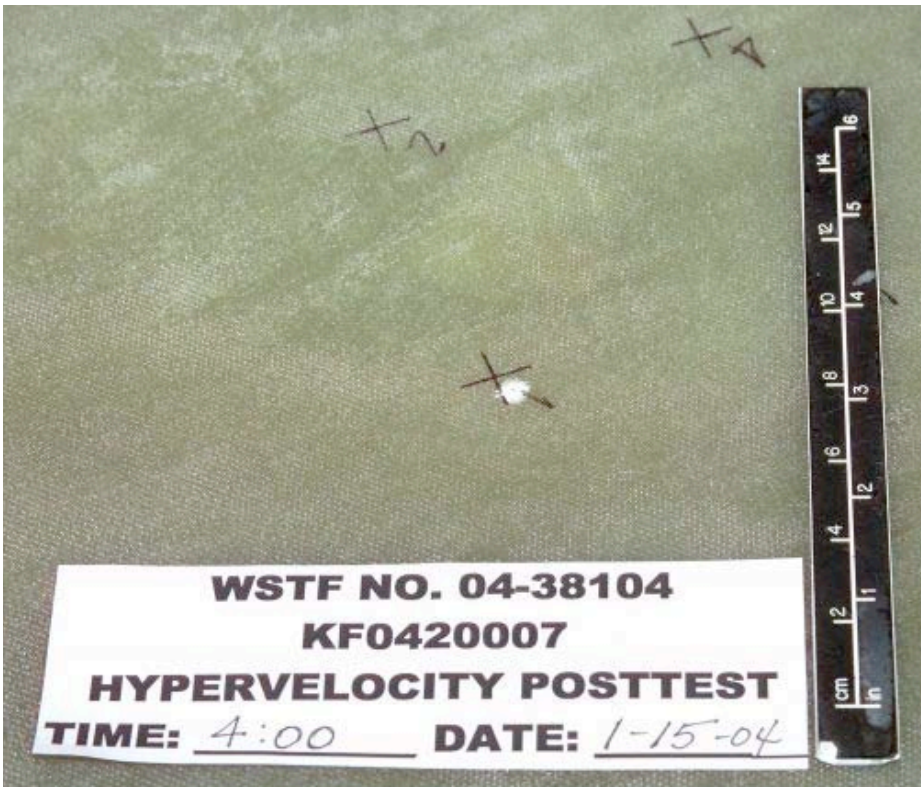

Figure 24: C-1 Shot #1 Impact Damage

Test conditions for AE (ultrasonic) data acquisition during hypervelocity impact testing

Test date: 1-20-04

Specimen description: Fiberglass
Target C-1
Shot # 2b

Impact conditions:
Projectile material and diameter: 0.6 mm diameter aluminum
Planned impact coordinates (in.): 15, 16
Actual impact coordinates (in.): 14.7, 16.2
AE estimated impact coordinates (in.):
Planned impact velocity (km/s): 6.8
Actual impact velocity (km/s): 7.0
Impact angle: 0

Sensor information:

Ch. #	Sensor Model	x coord. (in.)	y coord. (in.)	Attenuation at sensor * (dB)	Preamp gain/ attenuation (dB)	System gain (dB)	Total gain/ attenuation (dB)
1	225	10	7	-50	0	27	-23
2	225	24	7	-50	0	27	-23
3	225	10	27	-50	0	27	-23
4	225	24	27	-50	0	27	-23

* Preliminary estimate for attenuation at sensor based on field measurements. Attenuators calibrated for 50 ohm input, but used for high impedance preamp input. Further laboratory characterization required.

Signal filter settings: 20kHz – 1500 kHz bandpass on all channels
Instrumentation settings:
5 MHz sampling rate
32k points
4096 pretrigger points

Comments: Good signals acquired. Impact test 2 did not strike target, so 2b was a repeat of shot 2.

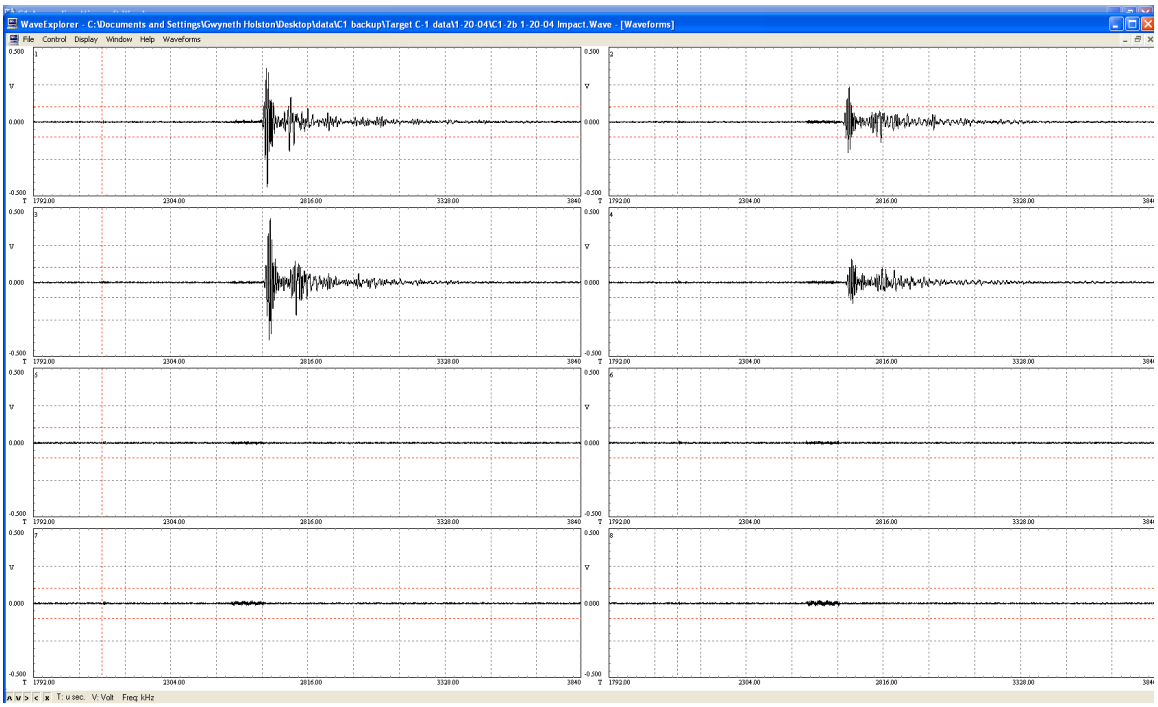

Figure 25: C-1 Shot #2b Impact Waveform

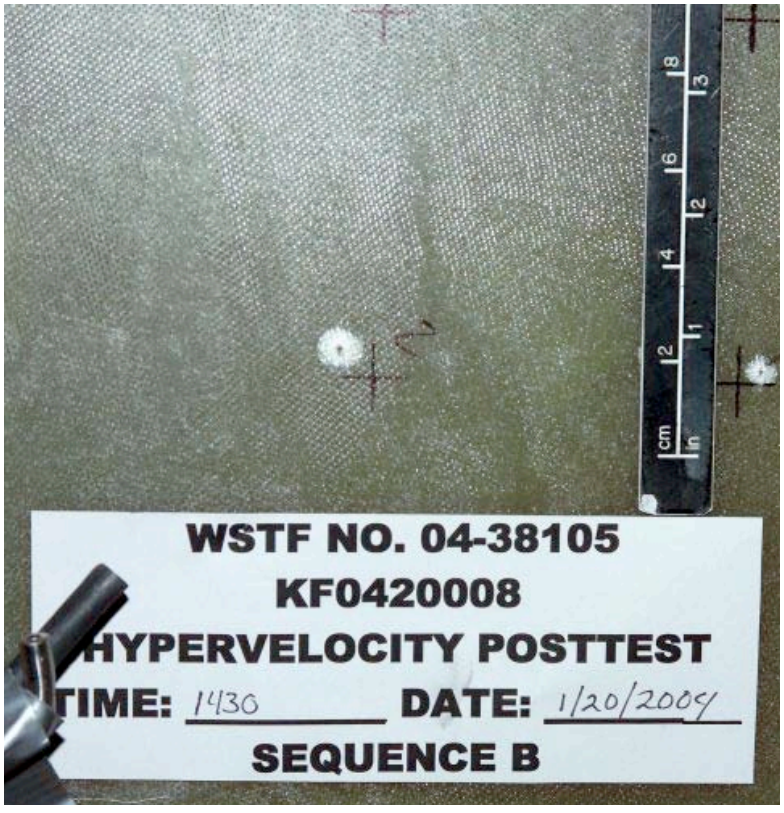

Figure 26: C-1 Shot #2b Impact Damage

Test conditions for AE (ultrasonic) data acquisition during hypervelocity impact testing

Test date: 1-21-04

Specimen description: Fiberglass
Target C-1
Shot # 3b

Impact conditions:
Projectile material and diameter: 0.4 mm diameter aluminum
Planned impact coordinates (in.): 21, 16
Actual impact coordinates (in.): 21.3, 16.3
AE estimated impact coordinates (in.):
Planned impact velocity (km/s): 6.8
Actual impact velocity (km/s): 6.94
Impact angle: 0

Sensor information:

Ch. #	Sensor Model	x coord. (in.)	y coord. (in.)	Attenuation at sensor * (dB)	Preamp gain/ attenuation (dB)	System gain (dB)	Total gain/ attenuation (dB)
1	225	10	7	-50	0	27	-23
2	225	24	7	-50	0	27	-23
3	225	10	27	-50	0	27	-23
4	225	24	27	-50	0	27	-23

* Preliminary estimate for attenuation at sensor based on field measurements.
Attenuators calibrated for 50 ohm input, but used for high impedance preamp input.
Further laboratory characterization required.

Signal filter settings: 20kHz – 1500 kHz bandpass on all channels
Instrumentation settings:
5 MHz sampling rate
32k points
4096 pretrigger points

Comments: Good signals acquired.

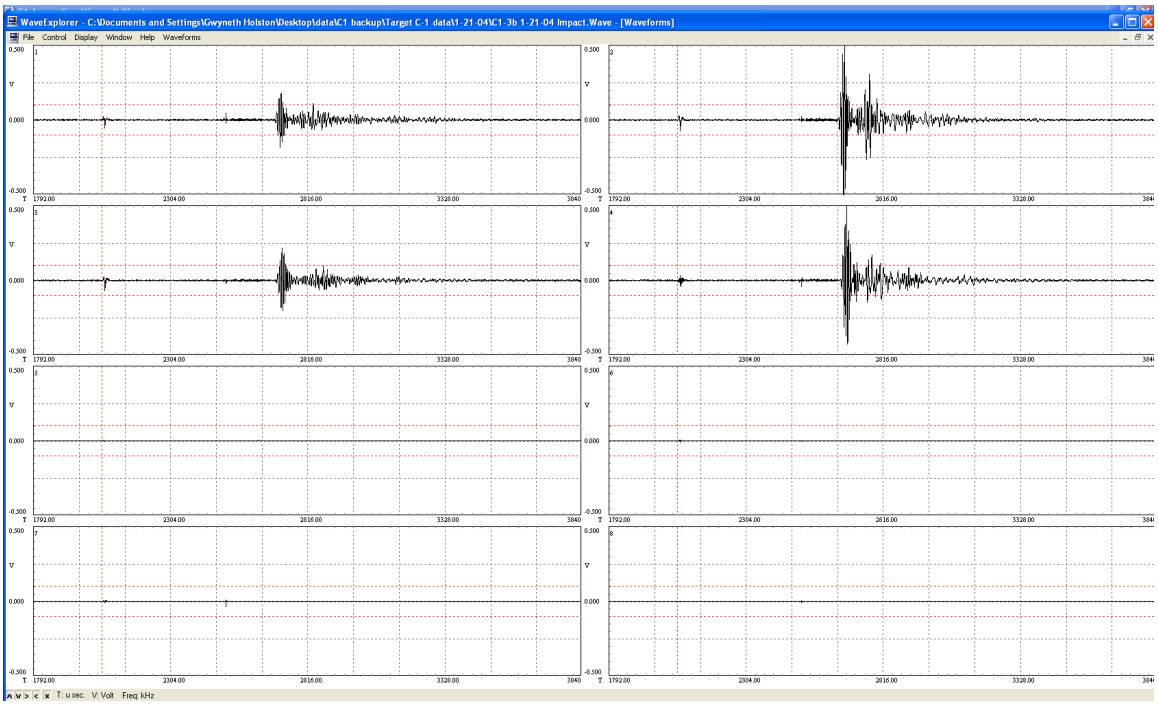

Figure 27: C-1 Shot #3b Impact Waveform

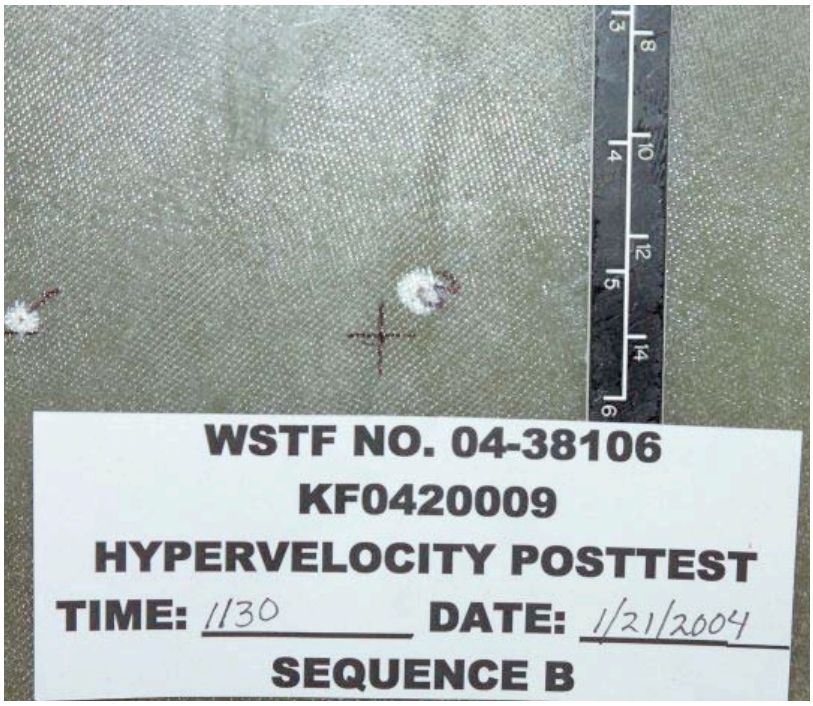

Figure 28: C-1 Shot #3b Impact Damage

Test conditions for AE (ultrasonic) data acquisition during hypervelocity impact testing

Test date: 1-21-04

Specimen description: Fiberglass
Target C-1
Shot # 4

Impact conditions:
Projectile material and diameter: 0.6 mm diameter aluminum
Planned impact coordinates (in.): 15, 19
Actual impact coordinates (in.): 15.2, 18.8
AE estimated impact coordinates (in.):
Planned impact velocity (km/s): 6.8
Actual impact velocity (km/s): 6.97
Impact angle: 0

Sensor information:

Ch. #	Sensor Model	x coord. (in.)	y coord. (in.)	Attenuation at sensor * (dB)	Preamp gain/ attenuation (dB)	System gain (dB)	Total gain/ attenuation (dB)
1	225	10	7	-50	0	27	-23
2	225	24	7	-50	0	27	-23
3	225	10	27	-50	0	27	-23
4	225	24	27	-50	0	27	-23

* Preliminary estimate for attenuation at sensor based on field measurements.
Attenuators calibrated for 50 ohm input, but used for high impedance preamp input.
Further laboratory characterization required.

Signal filter settings: 20kHz – 1500 kHz bandpass on all channels
Instrumentation settings:
5 MHz sampling rate
32k points
4096 pretrigger points

Comments: Good signals acquired.

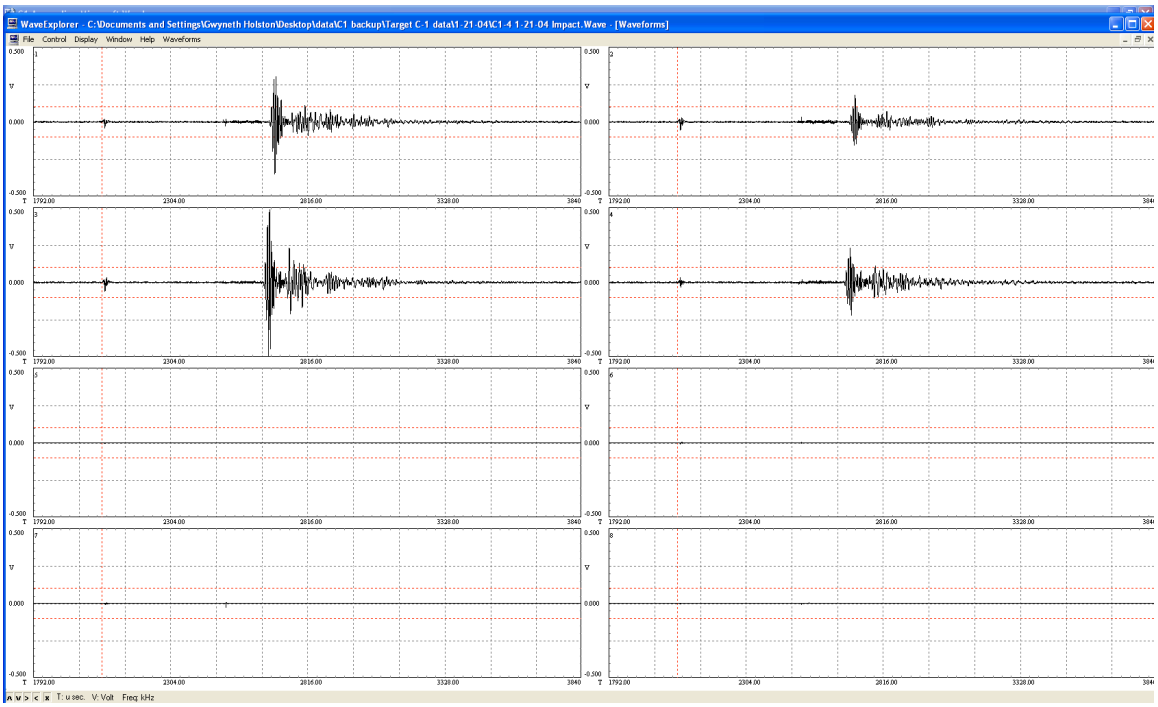

Figure 29: C-1 Shot #4 Impact Waveform

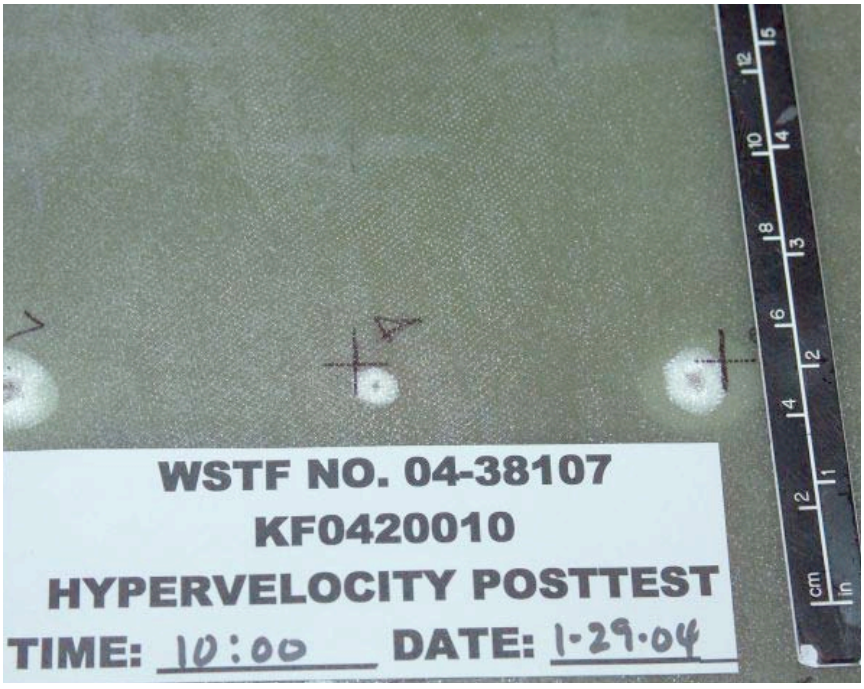

Figure 30: C-1 Shot #4 Impact Damage

Test conditions for AE (ultrasonic) data acquisition during hypervelocity impact testing
Test date: 1-22-04

Specimen description: Fiberglass
Target C-1
Shot # 5

Impact conditions:
Projectile material and diameter: 0.8 mm diameter aluminum
Planned impact coordinates (in.): 21, 19
Actual impact coordinates (in.): 21.1, 19.0
AE estimated impact coordinates (in.):
Planned impact velocity (km/s): 6.8
Actual impact velocity (km/s): 6.72
Impact angle: 0

Sensor information:

Ch. #	Sensor Model	x coord. (in.)	y coord. (in.)	Attenuation at sensor * (dB)	Preamp gain/ attenuation (dB)	System gain (dB)	Total gain/ attenuation (dB)
1	225	10	7	-50	0	18	-32
2	225	24	7	-50	0	18	-32
3	225	10	27	-50	0	18	-32
4	225	24	27	-50	0	18	-32

* Preliminary estimate for attenuation at sensor based on field measurements.
Attenuators calibrated for 50 ohm input, but used for high impedance preamp input.
Further laboratory characterization required.

Signal filter settings: 20kHz – 1500 kHz bandpass on all channels
Instrumentation settings:
5 MHz sampling rate
32k points
4096 pretrigger points

Comments: Good signals acquired.

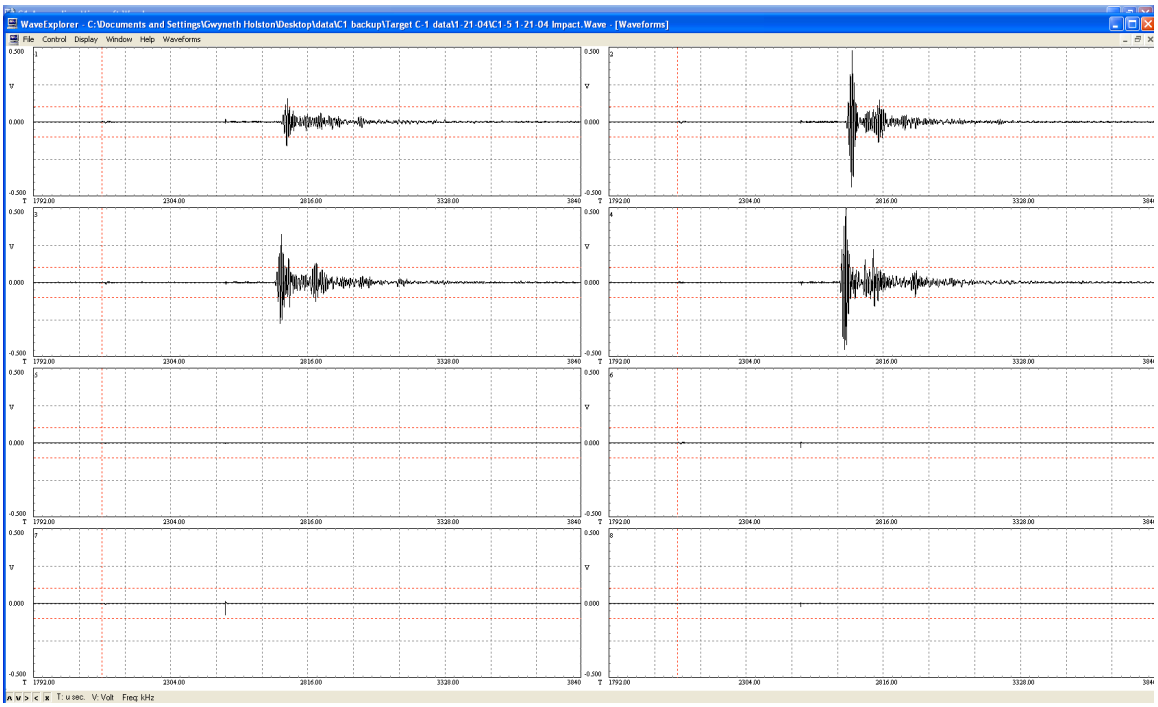

Figure 31: C-1 Shot #5 Impact Waveform

Figure 32: C-1 Shot #5 Impact Damage

Test conditions for AE (ultrasonic) data acquisition during hypervelocity impact testing

Test date: 1-22-04

Specimen description: Fiberglass
Target C-1
Shot # 6

Impact conditions:
Projectile material and diameter: 1.0 mm diameter aluminum
Planned impact coordinates (in.): 18, 19
Actual impact coordinates (in.): 17.8, 18.8
AE estimated impact coordinates (in.):
Planned impact velocity (km/s): 6.8
Actual impact velocity (km/s): 6.91
Impact angle: 0

Sensor information:

Ch. #	Sensor Model	x coord. (in.)	y coord. (in.)	Attenuation at sensor * (dB)	Preamp gain/ attenuation (dB)	System gain (dB)	Total gain/ attenuation (dB)
1	225	10	7	-50	0	12	-38
2	225	24	7	-50	0	12	-38
3	225	10	27	-50	0	12	-38
4	225	24	27	-50	0	12	-38

* Preliminary estimate for attenuation at sensor based on field measurements.
Attenuators calibrated for 50 ohm input, but used for high impedance preamp input.
Further laboratory characterization required.

Signal filter settings: 20kHz – 1500 kHz bandpass on all channels
Instrumentation settings:
5 MHz sampling rate
32k points
4096 pretrigger points

Comments: Good signals acquired.

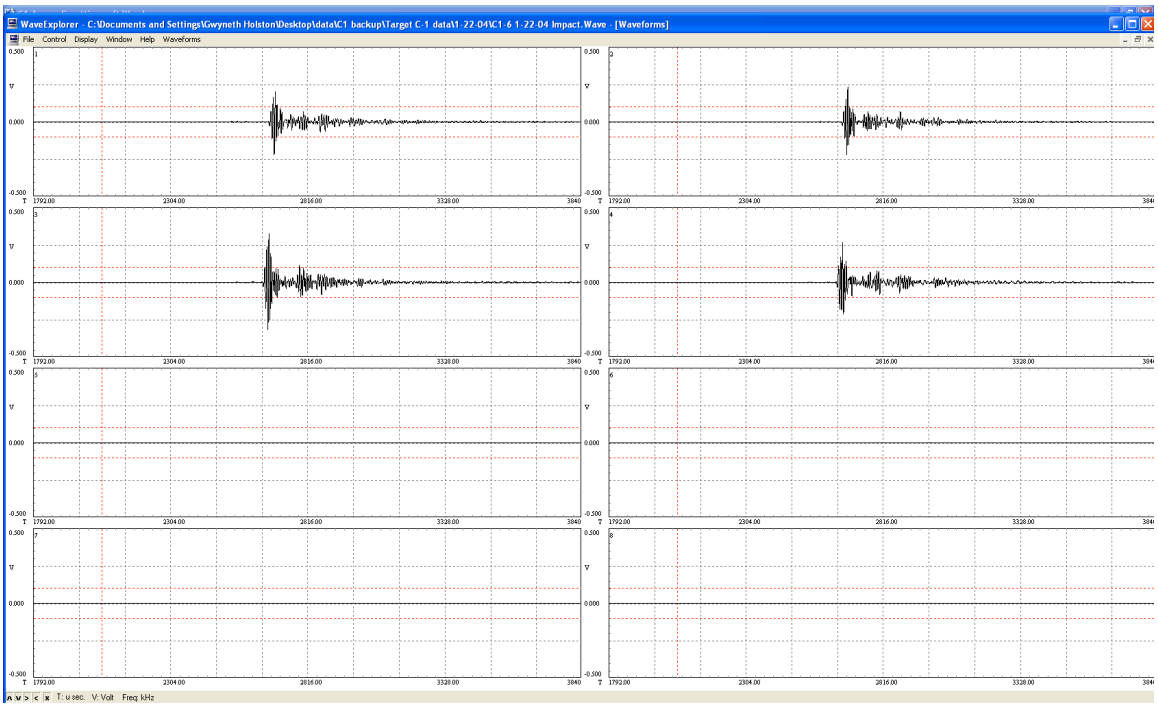

Figure 33: C-1 Shot #6 Impact Waveform

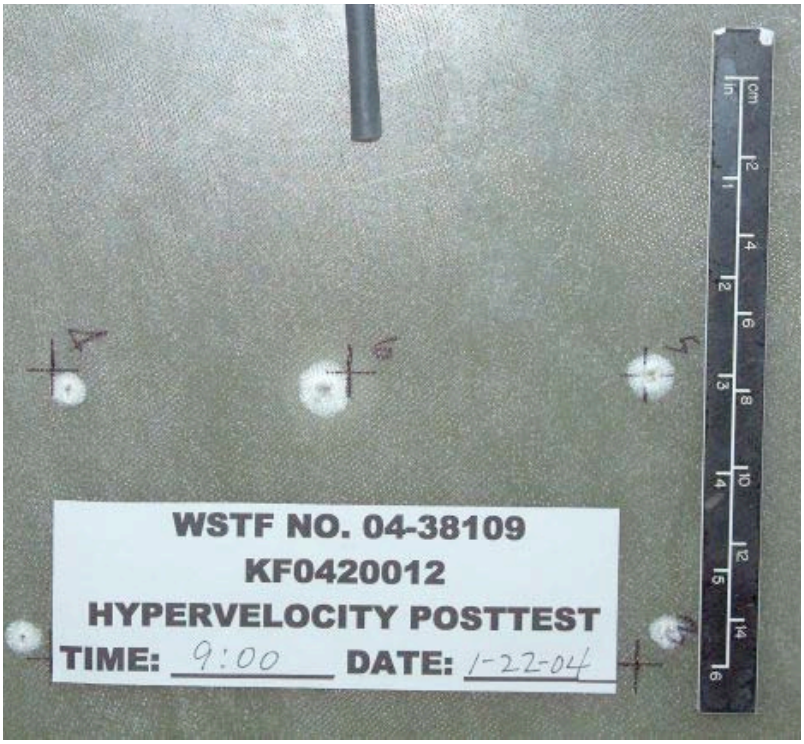

Figure 34: C-1 Shot #6 Impact Damage

Test conditions for AE (ultrasonic) data acquisition during hypervelocity impact testing

Test date: 1-22-04

Specimen description: Fiberglass
Target C-1
Shot # 7

Impact conditions:
Projectile material and diameter: 1.2 mm diameter aluminum
Planned impact coordinates (in.): 12, 19
Actual impact coordinates (in.): 12.2, 18.8
AE estimated impact coordinates (in.):
Planned impact velocity (km/s): 6.8
Actual impact velocity (km/s): 6.86
Impact angle: 0

Sensor information:

Ch. #	Sensor Model	x coord. (in.)	y coord. (in.)	Attenuation at sensor * (dB)	Preamp gain/ attenuation (dB)	System gain (dB)	Total gain/ attenuation (dB)
1	225	10	7	-50	0	9	-41
2	225	24	7	-50	0	9	-41
3	225	10	27	-50	0	9	-41
4	225	24	27	-50	0	9	-41

* Preliminary estimate for attenuation at sensor based on field measurements.
Attenuators calibrated for 50 ohm input, but used for high impedance preamp input.
Further laboratory characterization required.

Signal filter settings: 20kHz – 1500 kHz bandpass on all channels
Instrumentation settings:
5 MHz sampling rate
32k points
4096 pretrigger points

Comments: Good signals acquired.

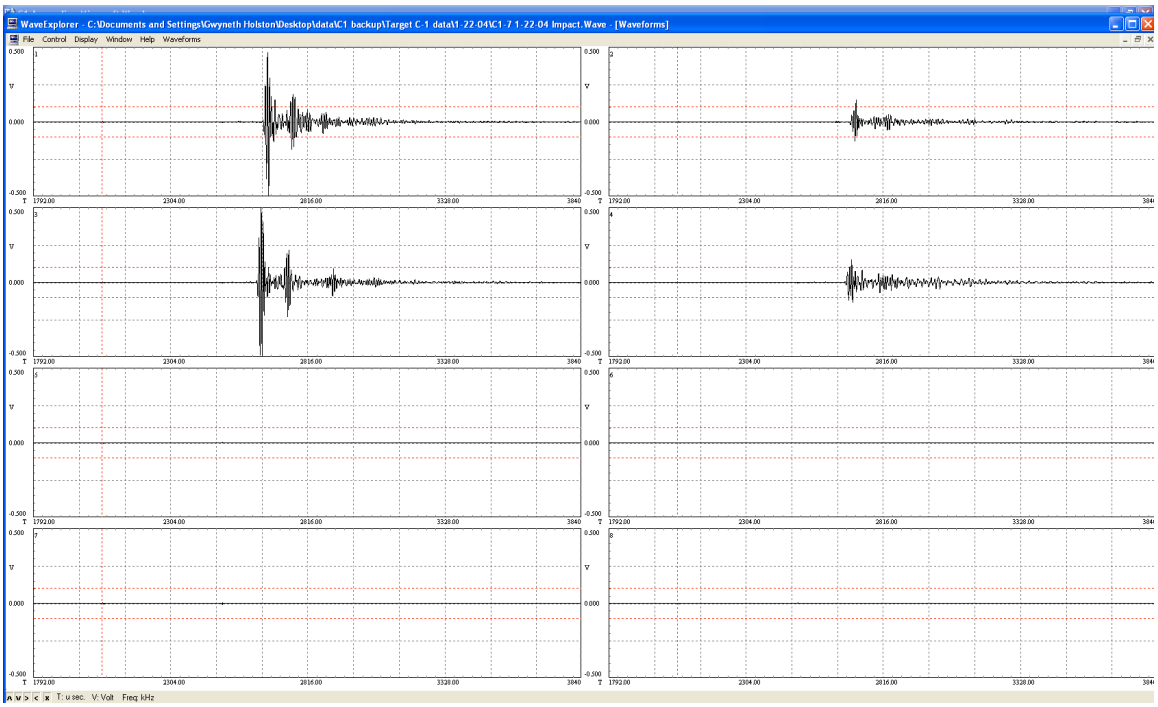

Figure 35: C-1 Shot #7 Impact Waveform

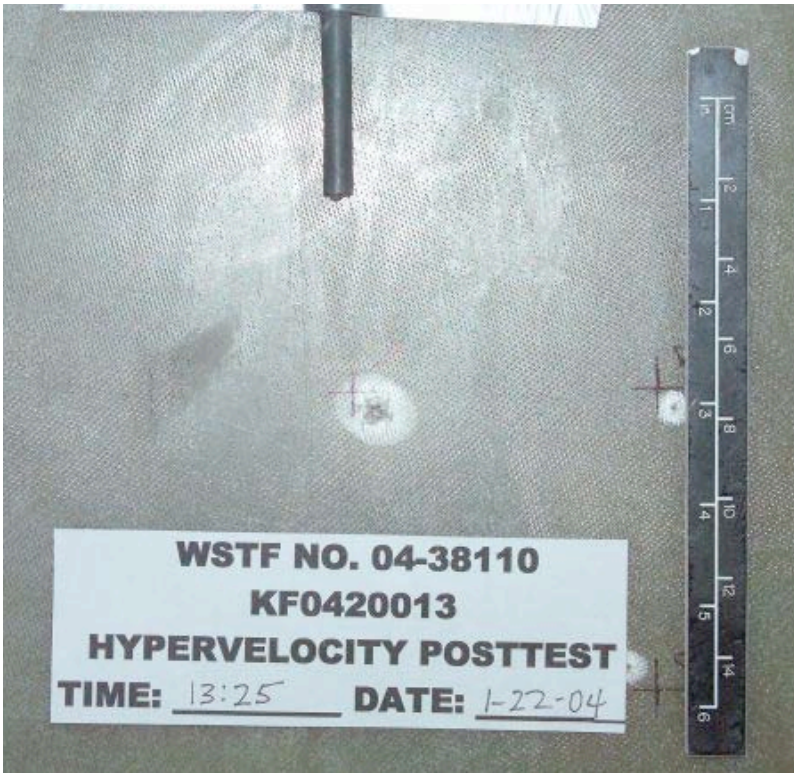

Figure 36: C-1 Shot #7 Impact Damage

Test conditions for AE (ultrasonic) data acquisition during hypervelocity impact testing

Test date: 1-22-04

Specimen description: Fiberglass
Target C-1
Shot # 8

Impact conditions:
Projectile material and diameter: 1.4 mm diameter aluminum
Planned impact coordinates (in.): 12, 15
Actual impact coordinates (in.): 11.8, 15.1
AE estimated impact coordinates (in.):
Planned impact velocity (km/s): 6.8
Actual impact velocity (km/s): 6.82
Impact angle: 0

Sensor information:

Ch. #	Sensor Model	x coord. (in.)	y coord. (in.)	Attenuation at sensor * (dB)	Preamp gain/ attenuation (dB)	System gain (dB)	Total gain/ attenuation (dB)
1	225	10	7	-50	0	6	-44
2	225	24	7	-50	0	6	-44
3	225	10	27	-50	0	6	-44
4	225	24	27	-50	0	6	-44

* Preliminary estimate for attenuation at sensor based on field measurements.
Attenuators calibrated for 50 ohm input, but used for high impedance preamp input.
Further laboratory characterization required.

Signal filter settings: 20kHz – 1500 kHz bandpass on all channels
Instrumentation settings:
5 MHz sampling rate
32k points
4096 pretrigger points

Comments: Good signals acquired.

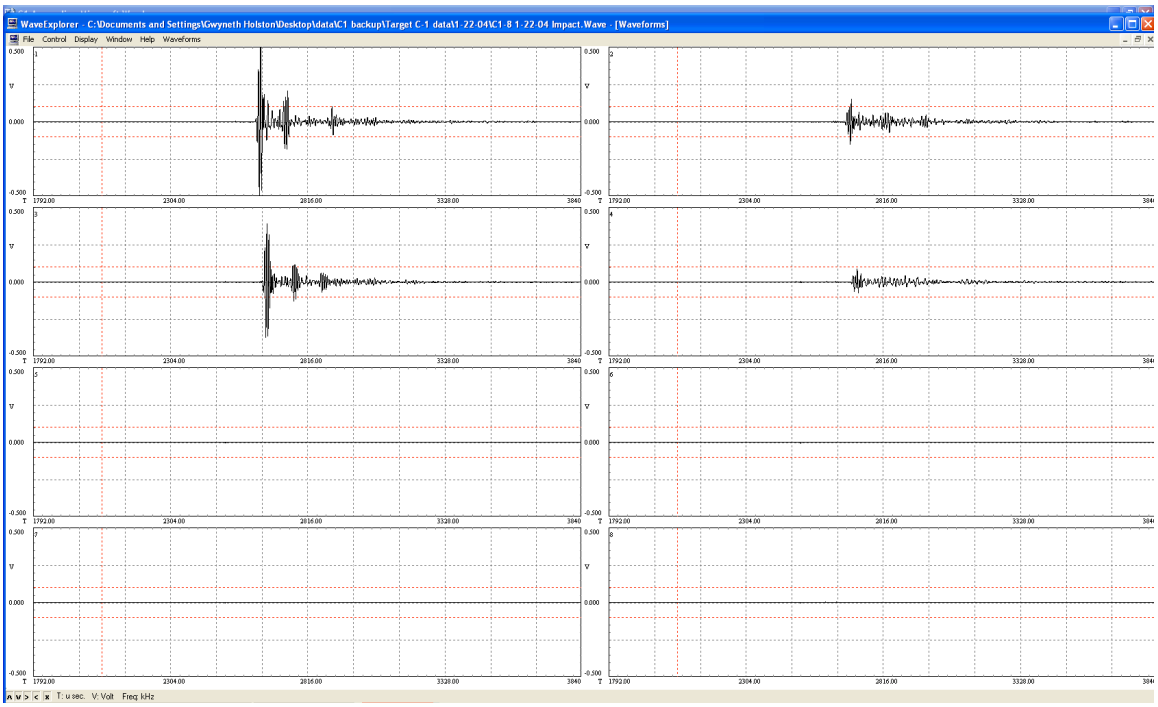

Figure 37: C-1 Shot #8 Impact Waveform

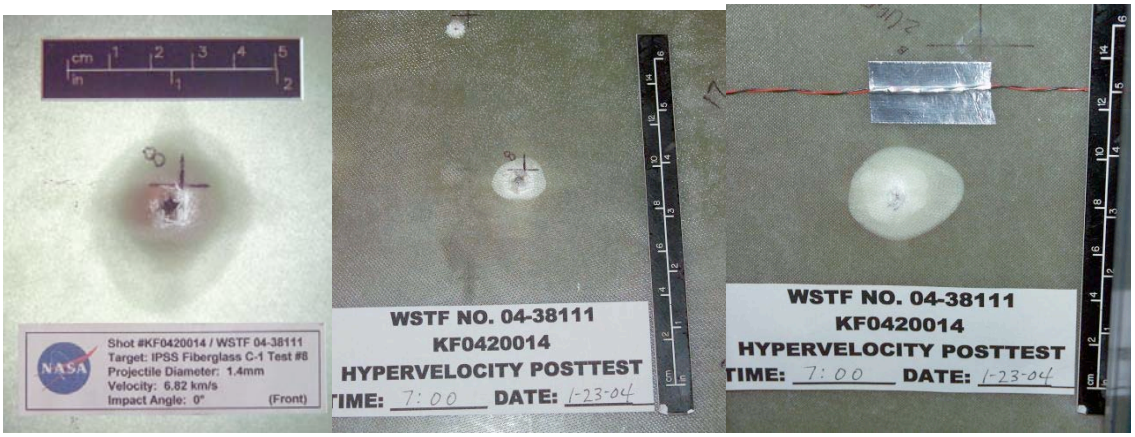

Figure 38: C-1 Shot #8 Impact Damage
(Left: Back Illuminated, Middle: Front View, Right: Back View)

Test conditions for AE (ultrasonic) data acquisition during hypervelocity impact testing

Test date: 1-23-04

Specimen description: Fiberglass
Target C-1
Shot # 9

Impact conditions:
Projectile material and diameter: 1.6 mm diameter aluminum
Planned impact coordinates (in.): 13, 12
Actual impact coordinates (in.): 12.9 , 11.8
AE estimated impact coordinates (in.):
Planned impact velocity (km/s): 6.8
Actual impact velocity (km/s): 6.95
Impact angle: 0

Sensor information:

Ch. #	Sensor Model	x coord. (in.)	y coord. (in.)	Attenuation at sensor * (dB)	Preamp gain/ attenuation (dB)	System gain (dB)	Total gain/ attenuation (dB)
1	225	10	7	-50	0	3	-47
2	225	24	7	-50	0	3	-47
3	225	10	27	-50	0	3	-47
4	225	24	27	-50	0	3	-47

* Preliminary estimate for attenuation at sensor based on field measurements.
Attenuators calibrated for 50 ohm input, but used for high impedance preamp input.
Further laboratory characterization required.

Signal filter settings: 20kHz – 1500 kHz bandpass on all channels
Instrumentation settings:
5 MHz sampling rate
32k points
4096 pretrigger points

Comments: Good signals acquired.

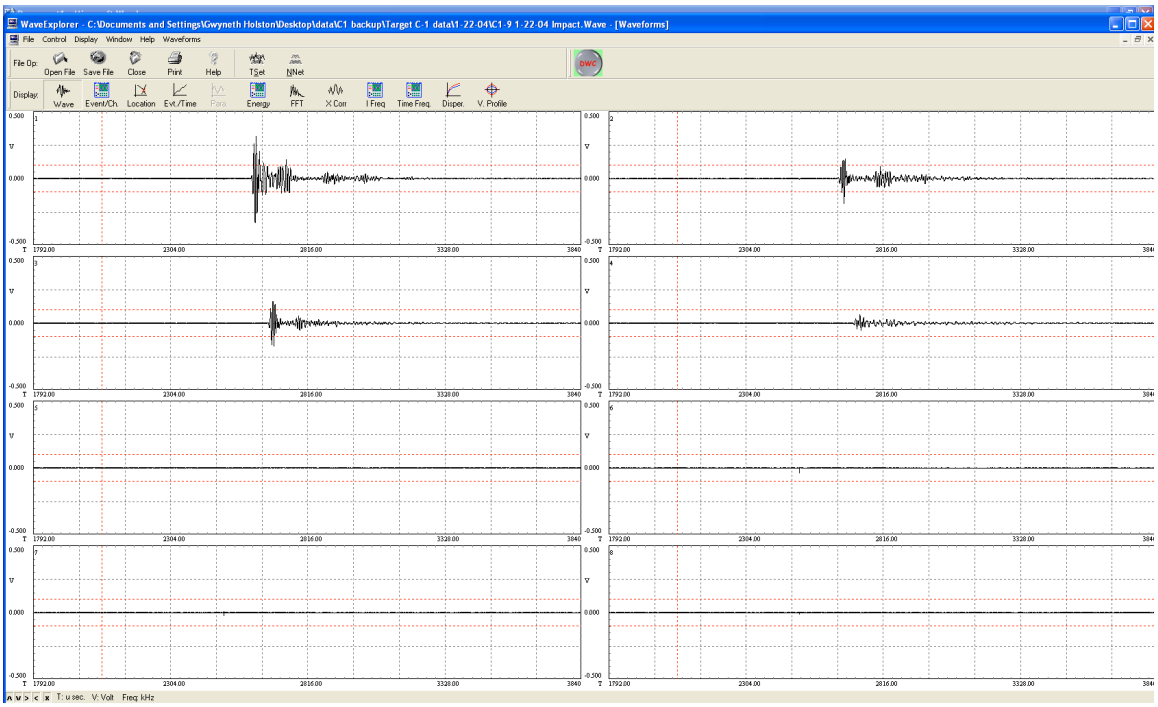

Figure 39: C-1 Shot #9 Impact Waveform

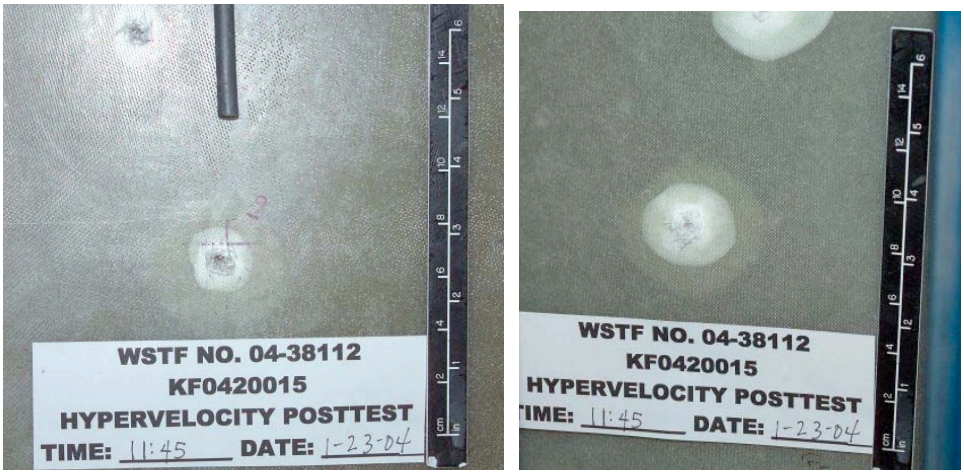

Figure 40: C-1 Shot #9 Impact Damage (Left: Front View, Right: Back View)

Test conditions for AE (ultrasonic) data acquisition during hypervelocity impact testing

Test date: 1-23-04

Specimen description: Fiberglass
Target C-1
Shot # 10

Impact conditions:
Projectile material and diameter: 2.0 mm diameter aluminum
Planned impact coordinates (in.): 17.5, 12
Actual impact coordinates (in.): 17.6 , 12.2
AE estimated impact coordinates (in.):
Planned impact velocity (km/s): 6.8
Actual impact velocity (km/s): 6.76
Impact angle: 0

Sensor information:

Ch. #	Sensor Model	x coord. (in.)	y coord. (in.)	Attenuation at sensor * (dB)	Preamp gain/ attenuation (dB)	System gain (dB)	Total gain/ attenuation (dB)
1	225	10	7	-50	0	3	-47
2	225	24	7	-50	0	3	-47
3	225	10	27	-50	0	3	-47
4	225	24	27	-50	0	3	-47

* Preliminary estimate for attenuation at sensor based on field measurements.
Attenuators calibrated for 50 ohm input, but used for high impedance preamp input.
Further laboratory characterization required.

Signal filter settings: 20kHz – 1500 kHz bandpass on all channels
Instrumentation settings:
5 MHz sampling rate
32k points
4096 pretrigger points

Comments: Good signals acquired.

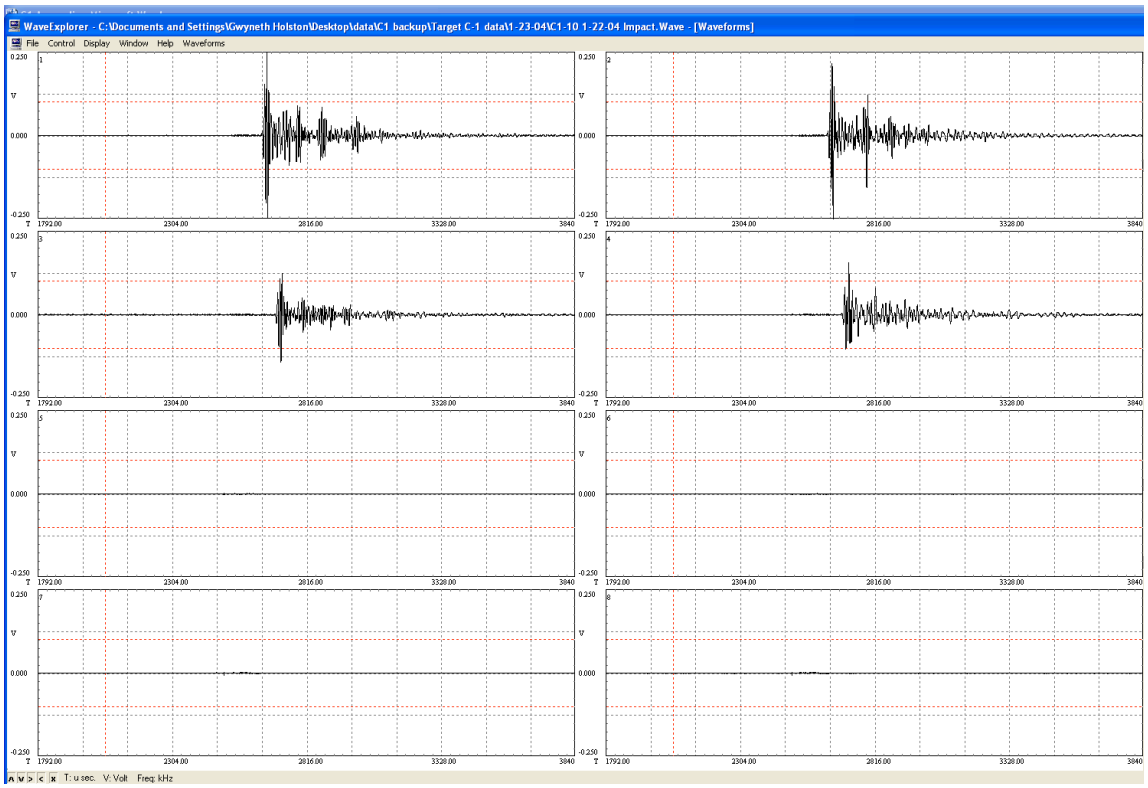

Figure 41: C-1 Shot #10 Impact Waveform

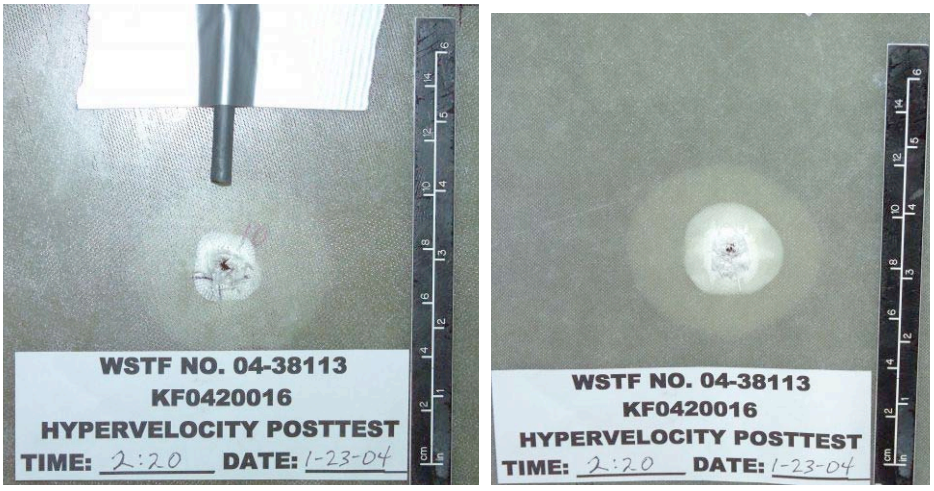

Figure 42: C-1 Shot #10 Impact Damage (Left: Front View, Right: Back View)

Test conditions for AE (ultrasonic) data acquisition during hypervelocity impact testing

Test date: 1-28-04

Specimen description: Fiberglass
Target C-1
Shot # 11

Impact conditions:
Projectile material and diameter: 0.8 mm diameter aluminum
Planned impact coordinates (in.): 14.5, 24
Actual impact coordinates (in.): 14.5, 24
AE estimated impact coordinates (in.):
Planned impact velocity (km/s): 6.8
Actual impact velocity (km/s): 6.91
Impact angle: 45

Sensor information:

Ch. #	Sensor Model	x coord. (in.)	y coord. (in.)	Attenuation at sensor * (dB)	Preamp gain/ attenuation (dB)	System gain (dB)	Total gain/ attenuation (dB)
1	225	10	7	-50	0	18	-32
2	225	24	7	-50	0	18	-32
3	225	10	27	-50	0	18	-32
4	225	24	27	-50	0	18	-32

* Preliminary estimate for attenuation at sensor based on field measurements.
Attenuators calibrated for 50 ohm input, but used for high impedance preamp input.
Further laboratory characterization required.

Signal filter settings: 20kHz – 1500 kHz bandpass on all channels
Instrumentation settings:
5 MHz sampling rate
32k points
4096 pretrigger points

Comments: Good signals acquired.

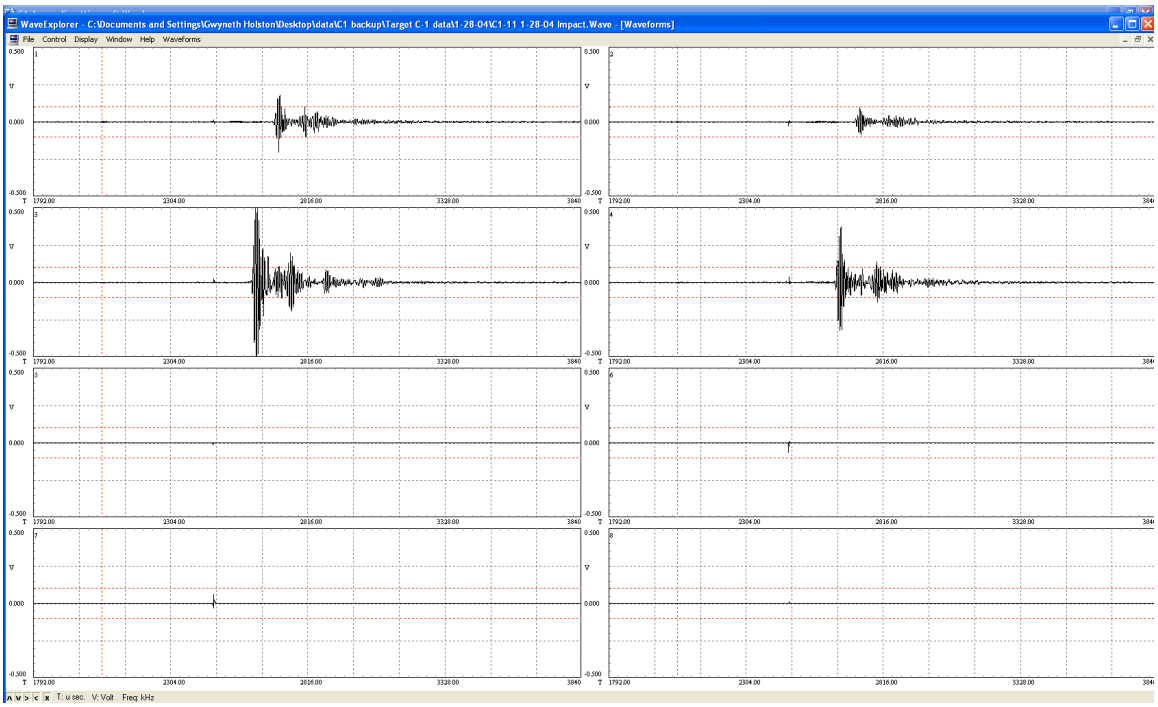

Figure 43: C-1 Shot #11 Impact Waveform

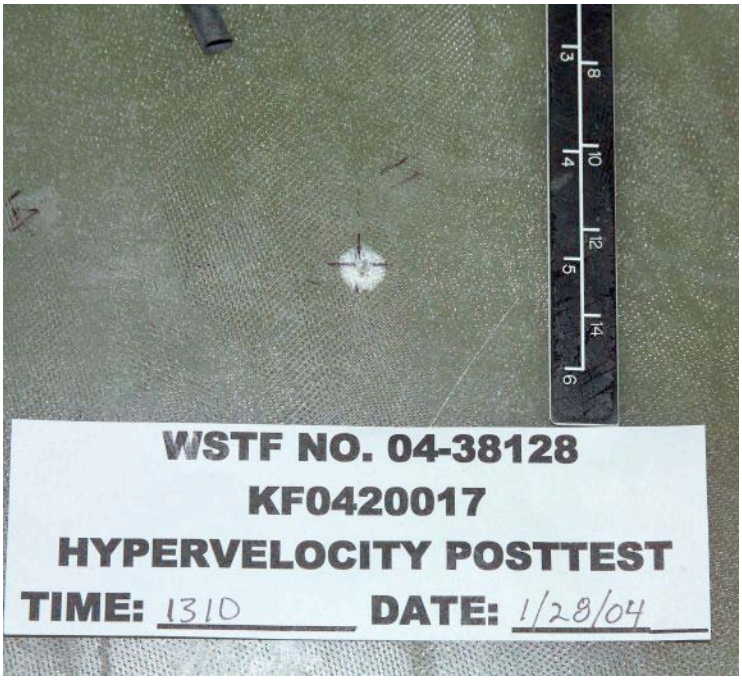

Figure 44: C-1 Shot #11 Impact Damage

Test conditions for AE (ultrasonic) data acquisition during hypervelocity impact testing

Test date: 1-28-04

Specimen description: Fiberglass
Target C-1
Shot # 12

Impact conditions:
Projectile material and diameter: 1.0 mm diameter aluminum
Planned impact coordinates (in.): 19.5, 24
Actual impact coordinates (in.): 19.7 , 24.1
AE estimated impact coordinates (in.):
Planned impact velocity (km/s): 6.8
Actual impact velocity (km/s): 6.64
Impact angle: 45

Sensor information:

Ch. #	Sensor Model	x coord. (in.)	y coord. (in.)	Attenuation at sensor * (dB)	Preamp gain/ attenuation (dB)	System gain (dB)	Total gain/ attenuation (dB)
1	225	10	7	-50	0	9	-41
2	225	24	7	-50	0	9	-41
3	225	10	27	-50	0	9	-41
4	225	24	27	-50	0	9	-41

* Preliminary estimate for attenuation at sensor based on field measurements.
Attenuators calibrated for 50 ohm input, but used for high impedance preamp input.
Further laboratory characterization required.

Signal filter settings: 20kHz – 1500 kHz bandpass on all channels
Instrumentation settings:
5 MHz sampling rate
32k points
4096 pretrigger points

Comments: Good signals acquired.

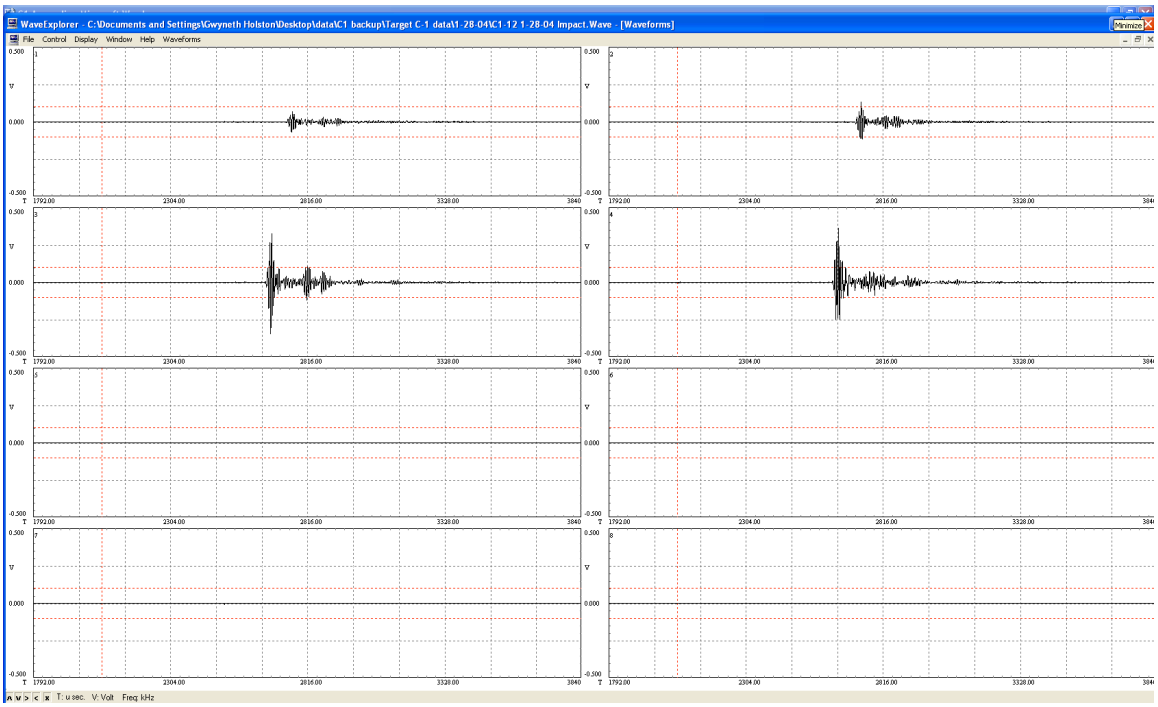

Figure 45: C-1 Shot #12 Impact Waveform

Figure 46: C-1 Shot #12 Impact Damage

Test conditions for AE (ultrasonic) data acquisition during hypervelocity impact testing

Test date: 1-29-04

Specimen description: Fiberglass
Target C-1
Shot # 13

Impact conditions:
Projectile material and diameter: 1.2 mm diameter aluminum
Planned impact coordinates (in.): 11 , 24
Actual impact coordinates (in.): 10.9 , 24.3
AE estimated impact coordinates (in.):
Planned impact velocity (km/s): 6.8
Actual impact velocity (km/s): 6.80
Impact angle: 45

Sensor information:

Ch. #	Sensor Model	x coord. (in.)	y coord. (in.)	Attenuation at sensor * (dB)	Preamp gain/ attenuation (dB)	System gain (dB)	Total gain/ attenuation (dB)
1	225	10	7	-50	0	9	-41
2	225	24	7	-50	0	9	-41
3	225	10	27	-50	0	9	-41
4	225	24	27	-50	0	9	-41

* Preliminary estimate for attenuation at sensor based on field measurements.
Attenuators calibrated for 50 ohm input, but used for high impedance preamp input.
Further laboratory characterization required.

Signal filter settings: 20kHz – 1500 kHz bandpass on all channels
Instrumentation settings:
5 MHz sampling rate
32k points
4096 pretrigger points

Comments: Good signals acquired.

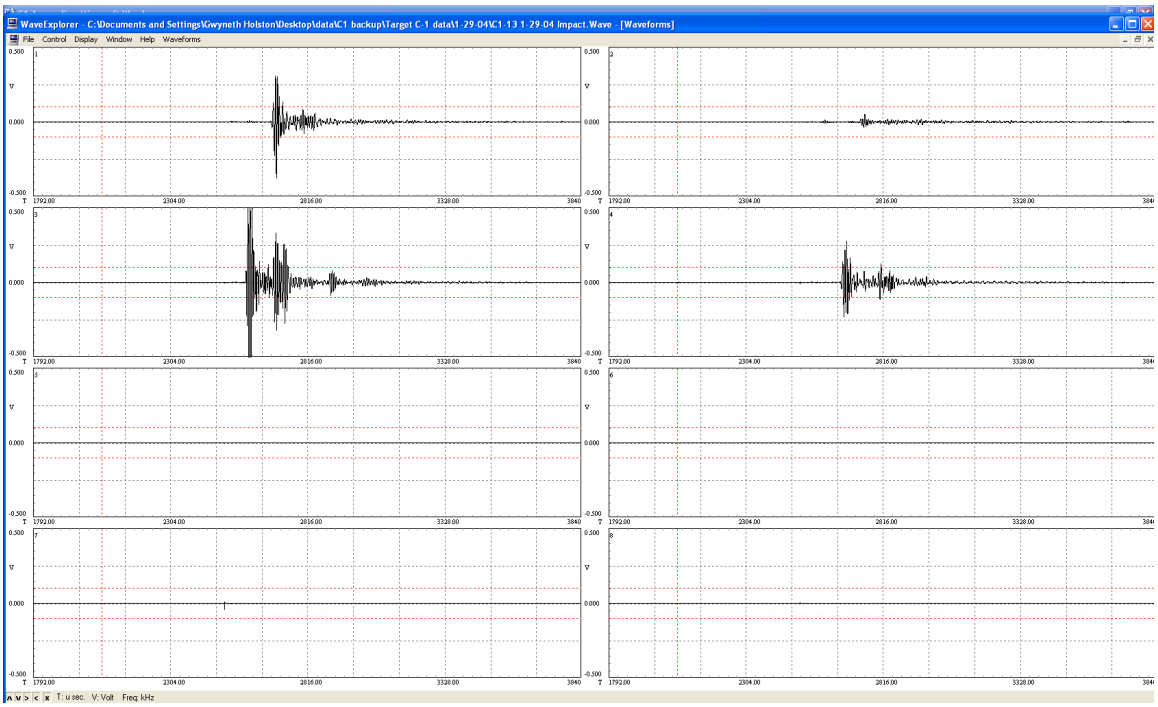

Figure 47: C-1 Shot #13 Impact Waveform

Figure 48: C-1 Shot #13 Impact Damage

Test conditions for AE (ultrasonic) data acquisition during hypervelocity impact testing

Test date: 1-29-04

Specimen description: Fiberglass
Target C-1
Shot # 14

Impact conditions:
Projectile material and diameter: 1.4 mm diameter aluminum
Planned impact coordinates (in.): 23 , 24
Actual impact coordinates (in.): 23.2 , 23.8
AE estimated impact coordinates (in.):
Planned impact velocity (km/s): 6.8
Actual impact velocity (km/s): 6.83
Impact angle: 45

Sensor information:

Ch. #	Sensor Model	x coord. (in.)	y coord. (in.)	Attenuation at sensor * (dB)	Preamp gain/ attenuation (dB)	System gain (dB)	Total gain/ attenuation (dB)
1	225	10	7	-50	0	6	-44
2	225	24	7	-50	0	6	-44
3	225	10	27	-50	0	6	-44
4	225	24	27	-50	0	6	-44

* Preliminary estimate for attenuation at sensor based on field measurements.
Attenuators calibrated for 50 ohm input, but used for high impedance preamp input.
Further laboratory characterization required.

Signal filter settings: 20kHz – 1500 kHz bandpass on all channels
Instrumentation settings:
5 MHz sampling rate
32k points
4096 pretrigger points

Comments: Good signals acquired.

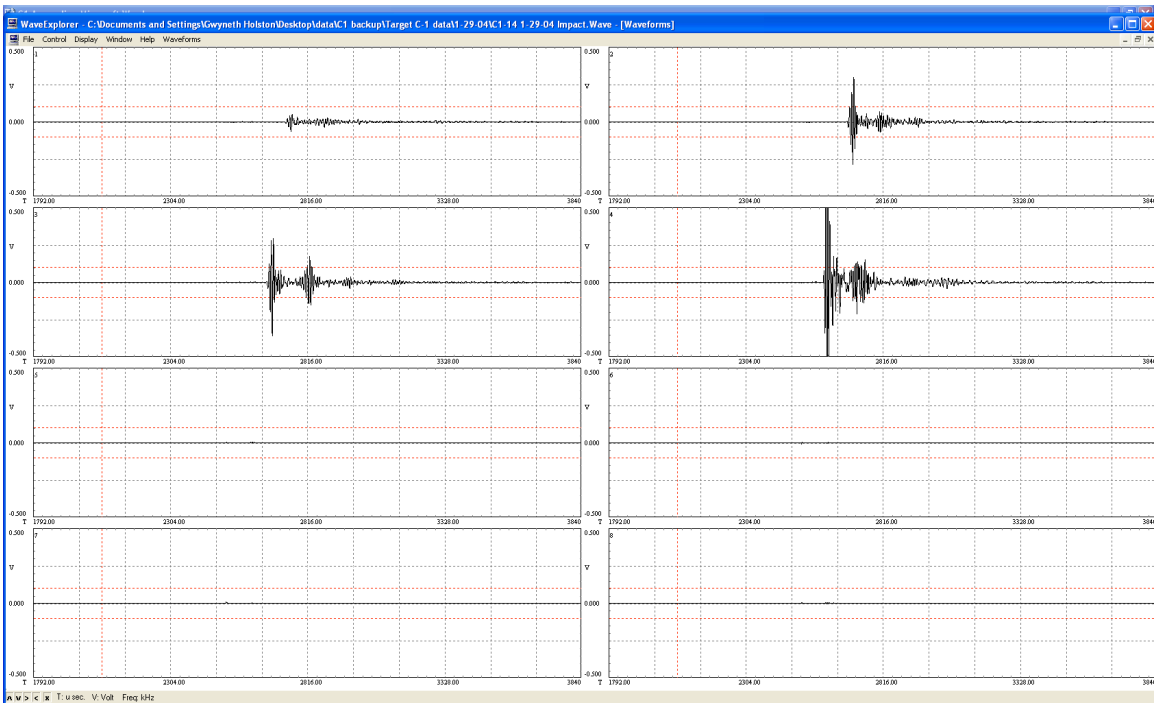

Figure 49: C-1 Shot #14 Impact Waveform

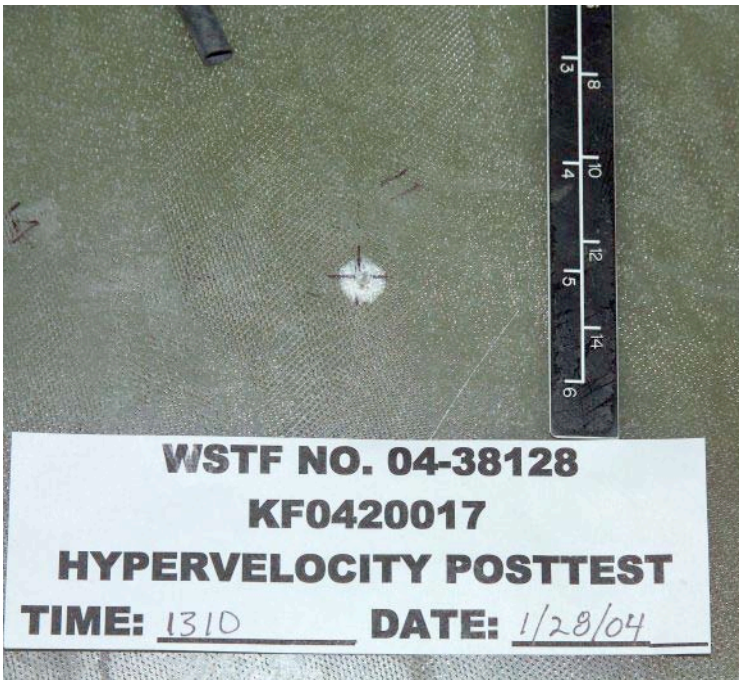

Figure 50: C-1 Shot #14 Impact Damage

Test conditions for AE (ultrasonic) data acquisition during hypervelocity impact testing

Test date: 2-2-04

Specimen description: Fiberglass
Target C-1
Shot # 15

Impact conditions:
Projectile material and diameter: 1.6 mm diameter aluminum
Planned impact coordinates (in.): 7 , 21
Actual impact coordinates (in.): 6.8 , 20.8
AE estimated impact coordinates (in.):
Planned impact velocity (km/s): 6.8
Actual impact velocity (km/s): 6.90
Impact angle: 45

Sensor information:

Ch. #	Sensor Model	x coord. (in.)	y coord. (in.)	Attenuation at sensor * (dB)	Preamp gain/ attenuation (dB)	System gain (dB)	Total gain/ attenuation (dB)
1	225	10	7	-50	0	3	-47
2	225	24	7	-50	0	3	-47
3	225	10	27	-50	0	3	-47
4	225	24	27	-50	0	3	-47

* Preliminary estimate for attenuation at sensor based on field measurements.
Attenuators calibrated for 50 ohm input, but used for high impedance preamp input.
Further laboratory characterization required.

Signal filter settings: 20kHz – 1500 kHz bandpass on all channels
Instrumentation settings:
5 MHz sampling rate
32k points
4096 pretrigger points

Comments: Signals not acquired, instrument not in record mode.

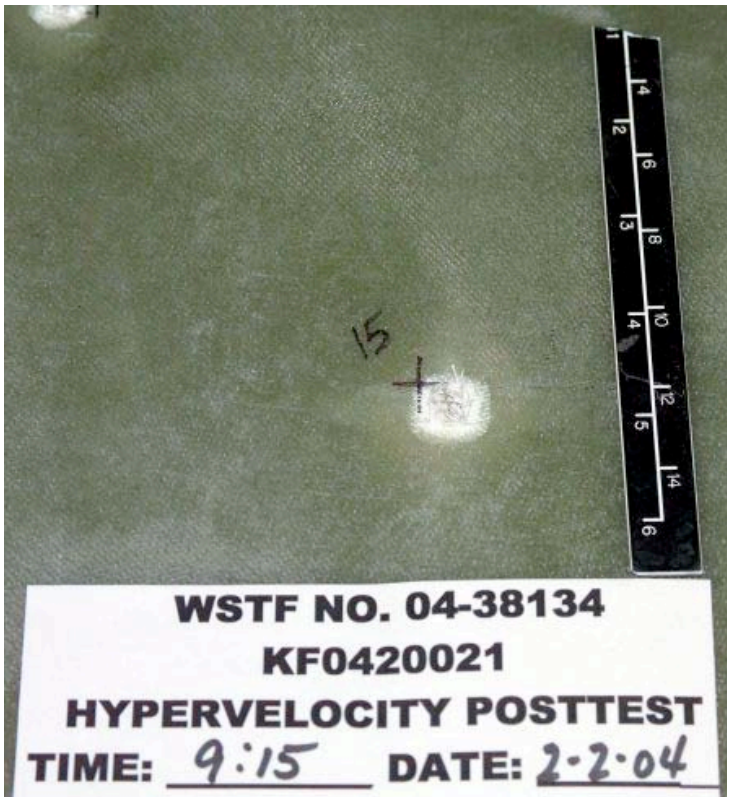

Figure 51: C-1 Shot #15 Impact Damage

Test conditions for AE (ultrasonic) data acquisition during hypervelocity impact testing

Test date: 2-2-04

Specimen description: Fiberglass
Target C-1
Shot # 16

Impact conditions:
Projectile material and diameter: 2.0 mm diameter aluminum
Planned impact coordinates (in.): 7 , 16
Actual impact coordinates (in.): 7 , 16
AE estimated impact coordinates (in.):
Planned impact velocity (km/s): 6.8
Actual impact velocity (km/s): 6.81
Impact angle: 45

Sensor information:

Ch. #	Sensor Model	x coord. (in.)	y coord. (in.)	Attenuation at sensor * (dB)	Preamp gain/ attenuation (dB)	System gain (dB)	Total gain/ attenuation (dB)
1	225	10	7	-50	0	3	-47
2	225	24	7	-50	0	3	-47
3	225	10	27	-50	0	3	-47
4	225	24	27	-50	0	3	-47

* Preliminary estimate for attenuation at sensor based on field measurements.
Attenuators calibrated for 50 ohm input, but used for high impedance preamp input.
Further laboratory characterization required.

Signal filter settings: 20kHz – 1500 kHz bandpass on all channels
Instrumentation settings:
5 MHz sampling rate
32k points
4096 pretrigger points

Comments: Good signals.

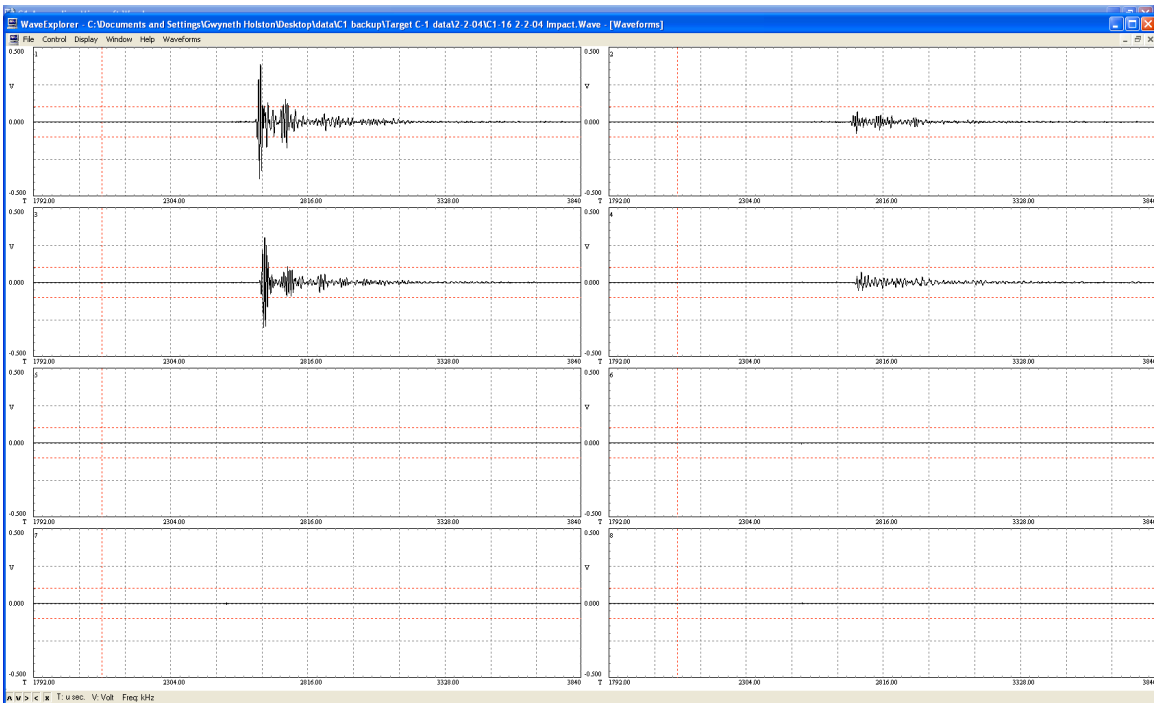

Figure 52: C-1 Shot #16 Impact Waveform

Figure 53: C-1 Shot #16 Impact Damage

Test conditions for AE (ultrasonic) data acquisition during hypervelocity impact testing

Test date: 2-2-04

Specimen description: Fiberglass
Target C-1
Shot # 17

Impact conditions:
Projectile material and diameter: 2.4 mm diameter aluminum
Planned impact coordinates (in.): 7 , 11.25
Actual impact coordinates (in.): 7.2 , 11.15
AE estimated impact coordinates (in.):
Planned impact velocity (km/s): 6.8
Actual impact velocity (km/s): 6.63
Impact angle: 45

Sensor information:

Ch. #	Sensor Model	x coord. (in.)	y coord. (in.)	Attenuation at sensor * (dB)	Preamp gain/ attenuation (dB)	System gain (dB)	Total gain/ attenuation (dB)
1	225	10	7	-50	-20	18	-52
2	225	24	7	-50	-20	18	-52
3	225	10	27	-50	-20	18	-52
4	225	24	27	-50	-20	18	-52

* Preliminary estimate for attenuation at sensor based on field measurements.
Attenuators calibrated for 50 ohm input, but used for high impedance preamp input.
Further laboratory characterization required.

Signal filter settings: 20kHz – 1500 kHz bandpass on all channels
Instrumentation settings:
5 MHz sampling rate
32k points
4096 pretrigger points

Comments: Good signals

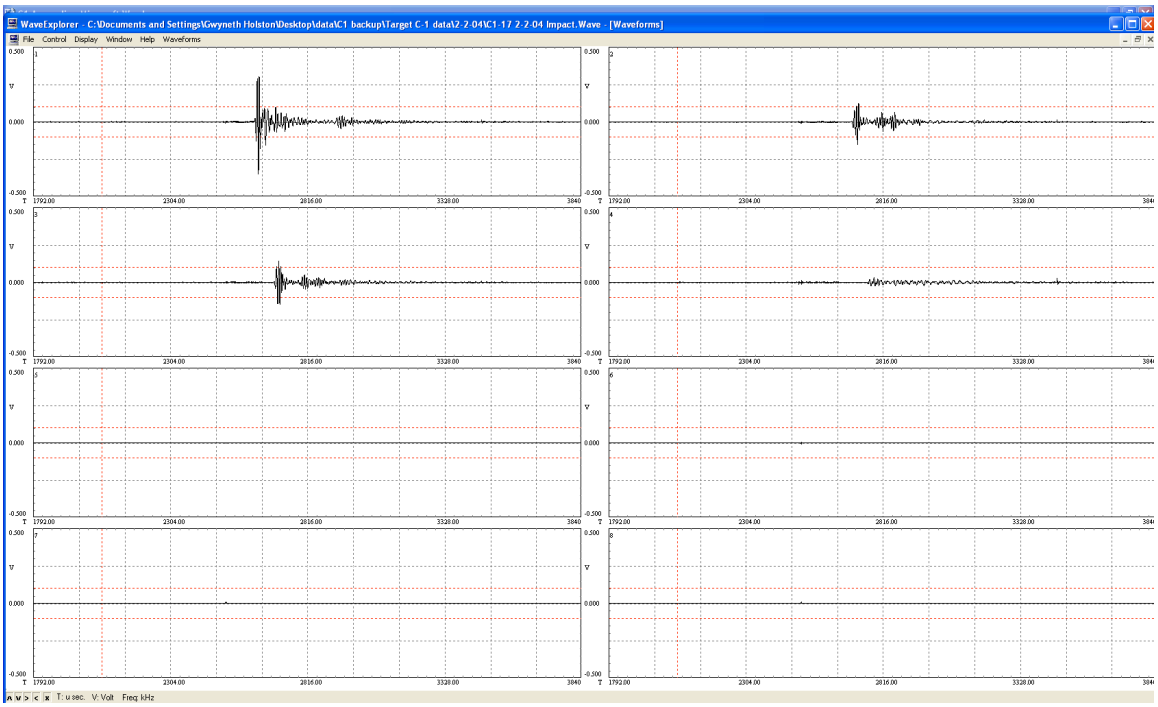

Figure 54: C-1 Shot #17 Impact Waveform

Figure 55: C-1 Shot #17 Impact Damage

Test conditions for AE (ultrasonic) data acquisition during hypervelocity impact testing

Test date: 2-3-04

Specimen description: Fiberglass
Target C-1
Shot # 18

Impact conditions:
Projectile material and diameter: 2.4 mm diameter aluminum
Planned impact coordinates (in.): 26 , 16
Actual impact coordinates (in.): 25.6 , 16.2
AE estimated impact coordinates (in.):
Planned impact velocity (km/s): 6.8
Actual impact velocity (km/s): 6.87
Impact angle: 45

Sensor information:

Ch. #	Sensor Model	x coord. (in.)	y coord. (in.)	Attenuation at sensor * (dB)	Preamp gain/ attenuation (dB)	System gain (dB)	Total gain/ attenuation (dB)
1	225	10	7	-50	-20	18	-52
2	225	24	7	-50	-20	18	-52
3	225	10	27	-50	-20	18	-52
4	225	24	27	-50	-20	18	-52

* Preliminary estimate for attenuation at sensor based on field measurements.
Attenuators calibrated for 50 ohm input, but used for high impedance preamp input.
Further laboratory characterization required.

Signal filter settings: 20kHz – 1500 kHz bandpass on all channels
Instrumentation settings:
5 MHz sampling rate
32k points
4096 pretrigger points

Comments: Good signals

No impact waveform available for C-1 shot #18.

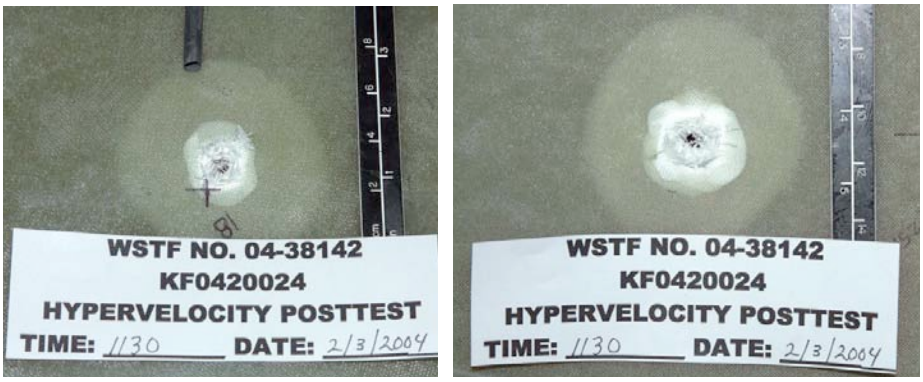

Figure 56: C-1 Shot #18 Impact Damage (Left: Front View, Right: Back View)

Test conditions for AE (ultrasonic) data acquisition during hypervelocity impact testing

Test date: 2-3-04

Specimen description: Fiberglass
Target C-1
Shot # 19

Impact conditions:
Projectile material and diameter: 2.0 mm diameter aluminum
Planned impact coordinates (in.): 26 , 11.25
Actual impact coordinates (in.): 25.4, 11.5
AE estimated impact coordinates (in.):
Planned impact velocity (km/s): 6.8
Actual impact velocity (km/s): 6.83
Impact angle: 45

Sensor information:

Ch. #	Sensor Model	x coord. (in.)	y coord. (in.)	Attenuation at sensor * (dB)	Preamp gain/ attenuation (dB)	System gain (dB)	Total gain/ attenuation (dB)
1	225	10	7	-50	0	3	-47
2	225	24	7	-50	0	3	-47
3	225	10	27	-50	0	3	-47
4	225	24	27	-50	0	3	-47

* Preliminary estimate for attenuation at sensor based on field measurements.
Attenuators calibrated for 50 ohm input, but used for high impedance preamp input.
Further laboratory characterization required.

Signal filter settings: 20kHz – 1500 kHz bandpass on all channels
Instrumentation settings:
5 MHz sampling rate
32k points
4096 pretrigger points

Comments: Good signals

No impact waveform available for C-1 shot #19.

No impact damage photo available for C-1 shot #19.

Data Tables

Test	Imp Dia	Imp Vel	Imp Ang	Normal K.E.	Total K.E.	Location		Channel Gain (dB)			
No.	mm	km/s	deg	J (± 5%)	J (± 5%)	x	y	1	2	3	4
C1-1	0.4	6.94	90	2.18	2.18	18.2	16.1	-23	-23	-23	-23
C1-2b	0.6	7.00	90	7.48	7.48	14.7	16.2	-23	-23	-23	-23
C1-3b	0.4	6.94	90	2.18	2.18	21.3	16.3	-23	-23	-23	-23
C1-4	0.6	6.97	90	7.42	7.42	15.2	18.8	-23	-23	-23	-23
C1-5	0.8	6.72	90	16.34	16.34	21.1	19	-32	-32	-32	-32
C1-6	1.0	6.91	90	33.75	33.75	17.8	18.8	-38	-38	-38	-38
C1-7	1.2	6.86	90	57.48	57.48	12.2	18.8	-41	-41	-41	-41
C1-8	1.4	6.82	90	90.22	90.22	11.8	15.1	-44	-44	-44	-44
C1-9	1.6	6.95	90	139.85	139.85	12.9	11.8	-47	-47	-47	-47
C1-10	2.0	6.76	90	258.41	258.41	17.6	12.2	-47	-47	-47	-47
C1-11	0.8	6.91	45	8.63	17.28	14.5	24	-32	-32	-32	-32
C1-12	1.0	6.64	45	15.57	31.17	19.7	24.1	-41	-41	-41	-41
C1-13	1.2	6.80	45	28.22	56.48	10.9	24.3	-41	-41	-41	-41
C1-14	1.4	6.83	45	45.20	90.48	23.2	23.8	-44	-44	-44	-44
C1-15	1.6	6.90	45	68.87	137.84	6.8	20.8	-47	-47	-47	-47
C1-16	2.0	6.81	45	131.02	262.25	7.0	16.0	-47	-47	-47	-47
C1-17	2.4	6.63	45	214.59	429.53	7.2	11.15	-52	-52	-52	-52
C1-18	2.4	6.87	45	230.41	461.19	25.6	16.2	-52	-52	-52	-52
C1-19	2.0	6.83	45	131.79	263.79	25.4	11.5	-47	-47	-47	-47

Table 3: C-1 Impactor Size, Impactor Velocity, Impactor Angle, Kinetic Energy, Actual Location, and Channel Gain

	Normal	Total	Crater Dims			Crater	Damage Dims		Damage
Test	K.E.	K.E.	x	y	z	Volume	x	y	Area
No.	J (± 5%)	J (± 5%)	mm	mm	mm	mm^3	mm	mm	mm^2
C1-1	2.18	2.18	1.3	0.7	0.5	0.5	2.0	2.0	4.0
C1-2b	7.48	7.48	1.5	1.4	1.0	2.1	3.5	2.5	8.8
C1-3b	2.18	2.18	1.7	2.0	1.5	5.1	3.5	5.0	17.5
C1-4	7.42	7.42	1.6	1.5	1.5	3.6	3.0	4.0	12.0
C1-5	16.34	16.34	1.9	1.8	2.0	6.8	5.0	4.5	22.5
C1-6	33.75	33.75	3.5	3.3	2.5	28.9	5.0	6.0	30.0
C1-7	57.48	57.48	4.5	4.0	3.0	54.0	8.0	8.0	64.0
C1-8	90.22	90.22	4.5	5.0	4.5	101.3	10.0	12.0	120.0
C1-9	139.85	139.85	5.5	5.0	4.8	132.7	13.0	13.0	169.0
C1-10	258.41	258.41	7.0	7.5	4.8	253.4	17.0	17.0	289.0
C1-11	8.63	17.28	2.1	2.6	1.0	5.5	4.0	4.4	17.6
C1-12	15.57	31.17	3.0	3.0	1.5	13.5	4.9	4.5	22.1
C1-13	28.22	56.48	4.7	3.9	2.0	36.7	7.4	6.3	46.6
C1-14	45.20	90.48	6.5	6.0	3.0	117.0	8.5	7.8	66.3
C1-15	68.87	137.84	8.0	6.0	4.0	192.0	9.7	9.0	87.3
C1-16	131.02	262.25	8.0	7.5	4.8	289.6	12.8	13.1	167.7
C1-17	214.59	429.53	9.0	7.5	4.8	325.8	14.1	14.7	207.3
C1-18	230.41	461.19	8.0	9.0	4.8	347.5	16.2	15.4	249.5
C1-19	131.79	263.79	6.5	8.0	4.8	251.0	14.0	13.4	187.6

Table 4: C-1 Normal Kinetic Energy, Total Kinetic Energy, Crater Damage Dimensions, Crater Damage Volume, Fiber Damage Dimensions, and Fiber Damage Area

	S1 RawEn	S2 RawEn	S3 RawEn	S4 RawEn	S1 En	S2 En	S3 En	S4 En	TOT WSE
	$Volts^2$-μs	$Volts^2$-μs	$Volts^2$-μs	$Volts^2$-μs	nJ	nJ	nJ	nJ	nJ
C1-1	0.150	0.247	0.111	0.199	2.997E+00	4.926E+00	2.222E+00	3.979E+00	1.412E+0
C1-2b	3.488	1.462	4.133	0.989	6.959E+01	2.918E+01	8.246E+01	1.972E+01	2.009E+0
C1-3b	0.570	3.294	0.675	2.620	1.137E+01	6.573E+01	1.346E+01	5.227E+01	1.428E+0
C1-4	1.320	0.392	2.923	0.821	2.634E+01	7.824E+00	5.832E+01	1.638E+01	1.089E+0
C1-5	0.354	1.962	1.265	2.748	5.606E+01	3.110E+02	2.005E+02	4.355E+02	1.003E+0
C1-6	0.547	0.533	1.161	0.756	3.450E+02	3.364E+02	7.328E+02	4.770E+02	1.891E+0
C1-7	2.338	0.213	2.808	0.383	2.944E+03	2.682E+02	3.535E+03	4.820E+02	7.229E+0
C1-8	2.608	0.308	1.510	0.138	6.552E+03	7.729E+02	3.793E+03	3.471E+02	1.147E+0
C1-9	1.345	0.357	0.323	0.075	6.743E+03	1.790E+03	1.621E+03	3.755E+02	1.053E+0
C1-10	0.791	0.680	0.239	0.310	3.963E+03	3.407E+03	1.200E+03	1.554E+03	1.012E+0
C1-11	0.474	0.133	4.188	1.561	7.507E+01	2.113E+01	6.638E+02	2.474E+02	1.007E+0
C1-12	0.073	0.184	1.059	1.045	9.185E+01	2.311E+02	1.333E+03	1.316E+03	2.972E+0
C1-13	1.148	0.037	5.656	0.890	1.445E+03	4.719E+01	7.121E+03	1.121E+03	9.734E+0
C1-14	0.062	0.694	1.179	4.308	1.567E+02	1.743E+03	2.961E+03	1.082E+04	1.568E+0
C1-15									
C1-16	1.642	0.112	1.095	0.121	8.231E+03	5.618E+02	5.486E+03	6.078E+02	1.489E+0
C1-17	0.992	0.234	0.261	0.046	1.572E+04	3.715E+03	4.129E+03	7.306E+02	2.429E+0
C1-18	0.075	0.365	0.082	0.636	1.187E+03	5.782E+03	1.307E+03	1.007E+04	1.835E+0
C1-19	0.459	0.335	0.069	0.437	2.298E+03	1.678E+03	3.460E+02	2.189E+03	6.512E+0

Table 5: C-1 Zeroed Raw Wave Signal, Channel Wave Signal Energy, Total Wave Signal Energy.
No signals were acquired for shot #15 because the system was not in record mode.

REPORT DOCUMENTATION PAGE

Form Approved
OMB No. 0704-0188

1. REPORT DATE *(DD-MM-YYYY)*	2. REPORT TYPE	3. DATES COVERED *(From - To)*
01- 09 - 2007	Contractor Report	

4. TITLE AND SUBTITLE
Hypervelocity Impact (HVI) - Volume 3: WLE Small-Scale Fiberglass Panel Flat Target C-1

5a. CONTRACT NUMBER
NNL05AC19T

5b. GRANT NUMBER

5c. PROGRAM ELEMENT NUMBER

6. AUTHOR(S)
Gorman, Michael R.; and Ziola, Steven M.

5d. PROJECT NUMBER

5e. TASK NUMBER

5f. WORK UNIT NUMBER
377816.06.03.03.06

7. PERFORMING ORGANIZATION NAME(S) AND ADDRESS(ES)
NASA Langley Research Center
Hampton, VA 23681-2199

8. PERFORMING ORGANIZATION REPORT NUMBER

9. SPONSORING/MONITORING AGENCY NAME(S) AND ADDRESS(ES)
National Aeronautics and Space Administration
Washington, DC 20546-0001

10. SPONSOR/MONITOR'S ACRONYM(S)
NASA

11. SPONSOR/MONITOR'S REPORT NUMBER(S)
NASA/CR-2007-214885/Vol3

12. DISTRIBUTION/AVAILABILITY STATEMENT
Unclassified - Unlimited
Subject Category 70
Availability: NASA CASI (301) 621-0390

13. SUPPLEMENTARY NOTES
Langley Technical Monitor: Eric I. Madaras
An electronic version can be found at http://ntrs.nasa.gov

14. ABSTRACT

During 2003 and 2004, the Johnson Space Center's White Sands Testing Facility in Las Cruces, New Mexico conducted hypervelocity impact tests on the space shuttle wing leading edge. Hypervelocity impact tests were conducted to determine if Micro-Meteoroid/Orbital Debris impacts could be reliably detected and located using simple passive ultrasonic methods. The objective of Target C-1 was to study hypervelocity impacts on the reinforced carbon-carbon (RCC) panels of the Wing Leading Edge. Fiberglass was used in place of RCC in the initial tests. Impact damage was detected using lightweight, low power instrumentation capable of being used in flight.

15. SUBJECT TERMS
Hypervelocity impact tests; Space shuttle; Wing leading edge; Debris; Impact damage

16. SECURITY CLASSIFICATION OF:			17. LIMITATION OF ABSTRACT	18. NUMBER OF PAGES	19a. NAME OF RESPONSIBLE PERSON
a. REPORT	b. ABSTRACT	c. THIS PAGE			STI Help Desk (email: help@sti.nasa.gov)
					19b. TELEPHONE NUMBER *(Include area code)*
U	U	U	UU	74	(301) 621-0390